NUMERICAL SOLUTION TO A LINEARIZED TIME FRACTIONAL KDV EQUATION ON UNBOUNDED DOMAINS

QIAN ZHANG, JIWEI ZHANG, SHIDONG JIANG, AND ZHIMIN ZHANG

ABSTRACT. An efficient numerical scheme is developed to solve a linearized time fractional KdV equation on unbounded spatial domains. First, the exact absorbing boundary conditions (ABCs) are derived which reduces the pure initial value problem into an equivalent initial boundary value problem on a finite interval that contains the compact support of the initial data and the inhomogeneous term. Second, the stability of the reduced initial-boundary value problem is studied in detail. Third, an efficient unconditionally stable finite difference scheme is constructed to solve the initial-boundary value problem where the nonlocal fractional derivative is evaluated via a sum-of-exponentials approximation for the convolution kernel. As compared with the direct method, the resulting algorithm reduces the storage requirement from $O(MN)$ to $O(M \log^d N)$ and the overall computational cost from $O(MN^2)$ to $O(MN \log^d N)$ with M the total number of spatial grid points and N the total number of time steps. Here $d = 1$ if the final time T is much greater than 1 and $d = 2$ if $T \approx 1$. Numerical examples are given to demonstrate the performance of the proposed numerical method.

1. INTRODUCTION

The classical Korteweg-de Vries (KdV) equation is a typical dispersive nonlinear partial differential equation (PDE). Historically, the solitary solution of the equation was first observed physically by Scott Russell in 1834 [27], and the equation itself was later derived by Korteweg and de Vries in 1895 [19]. Since then, it has been applied in many fields to describe a wide range of physical phenomena such as interaction of nonlinear waves [33], collision-free hydro-magnetic waves in a cold plasma, ion-acoustic waves, interfacial electrohydrodynamics [9], etc. As a mathematical model of the water wave, when the wave height is small compared to the water depth [32], the nonlinear equation is reduced to the linear KdV equation.

When these physical phenomena are considered nonconservative, they can be described using fractional differential equations. Over the last two decades the

fractional calculus has been applied to almost every field of science, engineering, and mathematics [18, 20, 22, 24, 25]. Here we consider the pure initial value problem (IVP) of the *linearized time fractional* KdV equation in one space dimension:

$$(1.1) \qquad \begin{cases} {}^{C}_{0}\mathcal{D}^{\alpha}_{t}u(x,t) + u_{xxx}(x,t) = f(x,t), \quad t \in (0,T], \ x \in \mathbb{R}, \\ u(x,0) = u_{0}(x), \qquad x \in \mathbb{R}, \\ u(x,t) \to 0, \quad \text{when } |x| \to \infty, \ t \in (0,T], \end{cases}$$

where the source term $f(x,t)$ and initial value $u_{0}(x)$ are assumed to be compactly supported, and the operator ${}^{C}_{0}\mathcal{D}^{\alpha}_{t}(0 < \alpha < 1)$ stands for the Caputo fractional derivative and is defined by the formula

$$(1.2) \qquad {}^{C}_{0}\mathcal{D}^{\alpha}_{t}u(x,t) = \frac{1}{\Gamma(1-\alpha)} \int_{0}^{t} \frac{u'(x,s)}{(t-s)^{\alpha}} \mathrm{d}s.$$

Although there are some methods to analytically solve the fractional KdV equation in some special cases [8, 23, 31, 35], one may have to resort to the numerical methods to obtain its solution in general. There are two difficulties when one tries to solve (1.1) numerically. First, the original problem is defined on the whole spatial domain, which has to be truncated to a finite domain for the purpose of numerical computation. For this, one needs to impose some artificial boundary conditions at the boundary of the truncated domain. These boundary conditions have to be carefully chosen so that there will be no reflections from the boundary and the reduced initial-boundary value problem (IBVP) is still stable and equals to the original problem in the truncated domain. Second, the fractional derivative is defined as a convolution integral from 0 to the current time t, and a direct method of evaluating the fractional derivative requires the storage of the solution at all times and quadratic complexity in computational cost, which is prohibitively expensive for large-scale long-time simulations.

Among these artificial boundary conditions, the so-called exact absorbing boundary conditions (ABCs) prevent the reflections of the wave from the boundary, which leads to an equivalent IBVP formulation for the original IVP. For the linearized KdV equation of the integer order, Zheng, Han, and Wen [37] derived the exact ABCs via the Laplace transform. Recently, Zhang, Li, and Wu [34] developed a series of high-order local ABCs to approximate the exact ABCs using Padé expansion in the Laplace domain. Besse et al. [5] constructed the discrete ABCs for the fully discrete problem using the $\mathcal{Z}$-transformation.

In this paper, we first derive exact ABCs for the linearized fractional KdV equation (1.1) with standard techniques in this field. That is, we apply the Laplace transform in time to reduce the equation to an ODE; we then use the condition that the solution has to decay to zero at infinity to obtain the solution of the ODE in the left and right exterior domains, which also leads to boundary conditions at two end points in the Laplace domain; the boundary conditions in the physical space are obtained by inverting back. However, unlike many second-order differential equations where only one boundary condition at each end point is needed, the KdV equation involves third order derivatives in space and one more boundary condition is required. All three absorbing boundary conditions are carefully chosen and we then show that the IBVP with our exact ABCs is stable in the L^{2}-norm.

Next, we construct a delicate finite difference (FD) scheme to discretize the IBVP. Our construction starts from the introduction of an auxillary variable which reduces

the third-order PDE to a second-order one. We then combine the PDE and the exact ABCs to obtain more consistent discrete equations for the boundary points. This way, we are able to show that the resulting FD scheme is unconditionally stable; whereas the naive FD schemes which discretize the spatial derivatives via central difference for interior points and one-sided differences for boundary points is only conditionally stable.

We further apply the fast algorithm in [15] to reduce the computational and storage cost for the evaluation of the fractional derivatives in the temporal variable. Here the main idea is to approximate the convolution kernel $t^{-1-\alpha}$ (obtained by integration by parts for the integral on the right-hand side of (1.2)) by a sum-of-exponentials (SOE) approximation when t is away from the origin. For each spatial point, the convolution with the exponential kernel can be evaluated in $O(1)$ time at each time step via standard recurrence relation or any A-stable ODE solver (see, for example, [2–4, 6, 12–15, 21, 36]). This reduces the computational cost from $O(N^2)$ for direct method to $O(NN_{\exp})$ and the storage cost from $O(N)$ for direct method to $O(N_{\exp})$, where N is the total number of time steps and $N_{\exp}$ is the total number of the exponentials needed in the SOE approximation. When similar SOE approximations are used for the exact ABCs as well, the overall computational cost of our algorithm is $O(MNN_{\exp})$ as compared with $O(MN^2)$ for direct method; and the storage requirement of our algorithm is $O(MN_{\exp})$ as compared with $O(MN)$ for direct method, as the direct method needs to store the solution in the whole computational spatial domain at all times. Here M is the total number of discretization points in space. The number of exponentials $N_{\exp}$ needed in the SOE approximation depends on the prescribed precision ε, the cutoff time step size δ, and the final time T. For a fixed absolute precision, $N_{\exp} = O(\log N)$ when $T \gg 1$ and $N_{\exp} = O(\log^2 N)$ when $T \approx 1$ if we assume that $N = \frac{T}{\delta}$, i.e., a uniform mesh is used in the temporal variable and the time step size is chosen to be $\Delta t = \delta$.

The rest of the paper is organized as follows. In section 2, we derive the exact ABCs for the linearized fractional KdV equation. In section 3, we present the stability analysis of the reduced IBVP. In section 4, we develop an efficient and stable finite difference scheme for solving the IBVP. Some numerical examples are given to demonstrate the performance of our scheme in section 5. Finally, we conclude our paper with a short summary.

2. The derivation of exact ABCs

We use the artificial boundary methods (ABMs) [11, 30] to construct the exact ABCs. We first introduce artificial boundaries $\Gamma_l := \{x | x = x_l\}$ and $\Gamma_r := \{x | x = x_r\}$ to divide the original infinite domain into three parts: the computational domain of interest $\Omega_c := (x_l, x_r)$, the left unbounded exterior domain $\Omega_l := (-\infty, x_l)$, and the right unbounded exterior domain $\Omega_r := (x_r, \infty)$. The choices of parameters x_l and x_r are determined such that the initial data $u_0(x)$ and the source term f are compactly supported in Ω_c. We consider the following two exterior problems on $\Omega_l := (-\infty, x_l)$ and $\Omega_r := (x_r, \infty)$, respectively:

$$(2.1) \qquad {}^{C}_{0}\mathcal{D}^{\alpha}_{t}u(x,t) + u_{xxx}(x,t) = 0, \qquad t \in (0, T],\ x \in \Omega_r,$$

$$(2.2) \qquad u(x,0) = 0, \qquad x \in \Omega_r,$$

$$(2.3) \qquad u(x,t) \to 0, \qquad \text{when } x \to +\infty,\ t \in (0, T],$$

and

(2.4) $$\qquad {}_{0}^{C}\mathcal{D}_{t}^{\alpha}u(x,t) + u_{xxx}(x,t) = 0, \qquad t \in (0,T], \ x \in \Omega_l,$$

(2.5) $$\qquad u(x,0) = 0, \qquad x \in \Omega_l,$$

(2.6) $$\qquad u(x,t) \to 0, \qquad \text{when } x \to -\infty, \ t \in (0,T].$$

We now derive certain conditions that must be satisfied for the solution u at the artificial boundaries x_l and x_r.

Let $\hat{u}(x,s)$ be the Laplace transform of $u(x,t)$ defined by

$$\hat{u}(x,s) = \int_{0}^{+\infty} e^{-st} u(x,t) \mathrm{d}t, \quad \Re(s) > 0.$$

The Laplace transform of the Caputo derivatives is given by the formula

$$\widehat{{}_{0}^{C}\mathcal{D}_{t}^{\alpha}u}(x,s) = s^{\alpha}\hat{u}(x,s) - s^{\alpha-1}u(x,0), \quad 0 < \alpha \le 1.$$

Applying the Laplace transform on equations (2.1) and (2.4) with zero initial values (2.2) and (2.5), we obtain an ODE in $\hat{u}(x,s)$:

(2.7) $$\qquad s^{\alpha}\hat{u}(x,s) + \hat{u}_{xxx}(x,s) = 0, \quad x \in \Omega_l \cup \Omega_r.$$

The general solution of (2.7) is given by the formula

(2.8) $$\qquad \hat{u}(x,s) = c_1(s)e^{\lambda_1(s)x} + c_2(s)e^{\lambda_2(s)x} + c_3(s)e^{\lambda_3(s)x},$$

where $\lambda_1(s), \lambda_2(s), \lambda_3(s)$ are the roots of the cubic equation

$$s^{\alpha} + \lambda^3 = 0.$$

That is,

(2.9) $$\qquad \lambda_1(s) = -s^{\frac{\alpha}{3}}, \ \lambda_2(s) = -s^{\frac{\alpha}{3}}\omega, \ \lambda_3(s) = -s^{\frac{\alpha}{3}}\omega^2$$

with $w = e^{2\pi i/3}$. It is easy to see that $\Re(\lambda_1(s)) < 0$, $\Re(\lambda_2(s)) > 0$, $\Re(\lambda_3(s)) > 0$.

Applying the Laplace transform on (2.3) and (2.6), we have

(2.10) $$\qquad \hat{u}(x,s) \to 0, \qquad \text{when} \qquad |x| \to \infty.$$

Thus, on the interval Ω_r,

$$\hat{u}(x,s) = c_1(s)e^{\lambda_1(s)x}.$$

Taking derivatives of this solution with respect to x, we obtain

(2.11) $$\qquad \hat{u}_{xx}(x,s) = \lambda_1^2(s)\hat{u}(x,s) \quad \text{and} \quad \hat{u}_x(x,s) = \lambda_1(s)\hat{u}(x,s)$$

or, equivalently,

(2.12) $$\qquad \frac{1}{\lambda_1^2(s)}\hat{u}_{xx}(x,s) = \hat{u}(x,s) \quad \text{and} \quad \frac{1}{\lambda_1(s)}\hat{u}_x(x,s) = \hat{u}(x,s).$$

Applying the inverse Laplace transform (see [25]) to (2.11) and (2.12) yields

(2.13) $$\qquad u_{xx}(x,t) = {}_{0}^{C}\mathcal{D}_{t}^{\frac{2\alpha}{3}}u(x,t) \quad \text{and} \quad u_x(x,t) = -{}_{0}^{C}\mathcal{D}_{t}^{\frac{\alpha}{3}}u(x,t),$$

(2.14) $$\qquad \mathcal{I}_{t}^{\frac{2\alpha}{3}}u_{xx}(x,t) = u(x,t) \quad \text{and} \quad \mathcal{I}_{t}^{\frac{\alpha}{3}}u_x(x,t) = -u(x,t),$$

where $\mathcal{I}_{t}^{\alpha}$ with $\alpha > 0$ is the Riemann-Liouville fractional integral defined by the formula

(2.15) $$\qquad \mathcal{I}_{t}^{\alpha}g(t) = \frac{1}{\Gamma(\alpha)} \int_{0}^{t} \frac{g(\tau)}{(t-\tau)^{1-\alpha}} \mathrm{d}\tau, \quad t > 0.$$

Similarly, on the interval Ω_l, we have $c_1 = 0$ from the decay condition (2.8) as $x \to -\infty$. Hence, the solution is

$$\hat{u}(x, s) = c_2(s)e^{\lambda_2(s)x} + c_3(s)e^{\lambda_3(s)x}.$$

Taking the first and second derivatives of $\hat{u}$ and eliminating c_2 and c_3, we obtain

$$\hat{u}_{xx}(x, s) - (\lambda_2 + \lambda_3)\hat{u}_x(x, s) + \lambda_2\lambda_3\hat{u}(x, s) = 0.$$

Using the facts that $\lambda_2 + \lambda_3 = -\lambda_1$ and $\lambda_2\lambda_3 = \lambda_1^2$, we have

$$(2.16) \qquad \hat{u}(x, s) + \frac{1}{\lambda_1(s)}\hat{u}_x(x, s) + \frac{1}{\lambda_1^2(s)}\hat{u}_{xx}(x, s) = 0$$

or, equivalently,

$$(2.17) \qquad \lambda_1^2(s)\hat{u}(x, s) + \lambda_1(s)\hat{u}_x(x, s) + \hat{u}_{xx}(x, s) = 0.$$

Applying the inverse Laplace transform to (2.16) and (2.17) leads to

$$(2.18) \qquad u(x, t) - \mathcal{I}_t^{\frac{\alpha}{3}} u_x(x, t) + \mathcal{I}_t^{\frac{2\alpha}{3}} u_{xx}(x, t) = 0,$$

$$(2.19) \qquad u_{xx}(x, t) - {}_0^C\mathcal{D}_t^{\frac{\alpha}{3}} u_x(x, t) + {}_0^C\mathcal{D}_t^{\frac{2\alpha}{3}} u(x, t) = 0.$$

Using (2.14) and (2.18) as exact artificial boundary conditions, the original IVP (1.1) is reduced to the the following IBVP on Ω_c:

$$(2.20) \qquad {}_0^C\mathcal{D}_t^\alpha u(x, t) + u_{xxx}(x, t) = f(x, t), \quad x \in \Omega_c, \ t \in (0, T],$$

$$(2.21) \qquad u(x, 0) = u_0(x), \qquad x \in \Omega_c,$$

$$(2.22) \qquad \mathcal{I}_t^{\frac{2\alpha}{3}} u_{xx}(x_r, t) = u(x_r, t),$$

$$(2.23) \qquad \mathcal{I}_t^{\frac{\alpha}{3}} u_x(x_r, t) = -u(x_r, t),$$

$$(2.24) \qquad \mathcal{I}_t^{\frac{2\alpha}{3}} u_{xx}(x_l, t) - \mathcal{I}_t^{\frac{\alpha}{3}} u_x(x_l, t) + u(x_l, t) = 0.$$

Similarly, using (2.13) and (2.19) as exact artificial boundary conditions, the original IVP (1.1) is reduced to the following IBVP on Ω_c:

$$(2.25) \qquad {}_0^C\mathcal{D}_t^\alpha u(x, t) + u_{xxx}(x, t) = f(x, t), \quad x \in \Omega_c, \ t \in (0, T],$$

$$(2.26) \qquad u(x, 0) = u_0(x), \qquad x \in \Omega_c,$$

$$(2.27) \qquad u_{xx}(x_r, t) = {}_0^C\mathcal{D}_t^{\frac{2\alpha}{3}} u(x_r, t),$$

$$(2.28) \qquad u_x(x_r, t) = -{}_0^C\mathcal{D}_t^{\frac{\alpha}{3}} u(x_r, t),$$

$$(2.29) \qquad u_{xx}(x_l, t) - {}_0^C\mathcal{D}_t^{\frac{\alpha}{3}} u_x(x_l, t) + {}_0^C\mathcal{D}_t^{\frac{2\alpha}{3}} u(x_l, t) = 0.$$

3. Stability of the exact absorbing boundary conditions

We now show that both the IBVP (2.20)–(2.24) and the IBVP (2.25)–(2.29) are stable in L^2-norm. We begin with some useful lemmas.

Lemma 3.1 (See [1]). *Suppose that $v(t)$ is absolutely continuous on $[0, T]$. Then*

$$v(t){}_0^C\mathcal{D}_t^\alpha v(t) \geq \frac{1}{2}{}_0^C\mathcal{D}_t^\alpha v^2(t), \quad 0 < \alpha < 1.$$

Lemma 3.2 (See [25]). *Suppose that $v(t)$ satisfies the inequality*

$$v(t) \leq a(t) + b(t) \int_0^t (t-s)^{\alpha-1} v(s) \mathrm{d}s, \quad \alpha > 0,$$

for $t \in [0, T]$, where $a(t)$ is not decreasing, nonnegative and locally integrable over $[0, T]$, and $b(t)$ is nonnegative and nondecreasing. Then

$$v(t) \leq a(t) E_\alpha(b(t)\Gamma(\alpha)t^\alpha), \quad 0 \leq t \leq T,$$

where $E_\alpha(z) = \sum_{n=0}^\infty \frac{z^n}{\Gamma(n\alpha+1)}$ is the Mittag-Leffler function.

Lemma 3.3. *Suppose that $y(t)$ is absolutely continuous on $[0, T]$. Then*

$$\mathcal{I}_t^1 {}_0^C \mathcal{D}_t^\alpha y(t) = -\frac{t^{1-\alpha}}{\Gamma(2-\alpha)} y(0) + \mathcal{I}_t^{1-\alpha} y(t).$$

Proof. Using the definitions for the Caputo fractional derivative (1.2) and Riemann-Liouville integral (2.15), we obtain

$$\mathcal{I}_t^1 {}_0^C \mathcal{D}_t^\alpha y(t) = \int_0^t \frac{1}{\Gamma(1-\alpha)} \int_0^\tau \frac{y'(\eta)}{(\tau-\eta)^\alpha} \mathrm{d}\eta \mathrm{d}\tau.$$

Exchanging the order of integration and performing integration by parts, we have

$$
\begin{aligned}
\mathcal{I}_t^1 {}_0^C \mathcal{D}_t^\alpha y(t) &= \frac{1}{\Gamma(1-\alpha)} \int_0^t y'(\eta) \int_\eta^t \frac{1}{(\tau-\eta)^\alpha} \mathrm{d}\tau \mathrm{d}\eta \\
&= \frac{1}{\Gamma(1-\alpha)(1-\alpha)} \int_0^t y'(\eta)(t-\eta)^{1-\alpha} \mathrm{d}\eta \\
&= -\frac{t^{1-\alpha}}{\Gamma(2-\alpha)} y(0) + \frac{1}{\Gamma(1-\alpha)} \int_0^t \frac{y(\eta)}{(t-\eta)^\alpha} \mathrm{d}\eta \\
&= -\frac{t^{1-\alpha}}{\Gamma(2-\alpha)} y(0) + \mathcal{I}_t^{1-\alpha} y(t),
\end{aligned}
$$

and the proof is complete. $\square$

Lemma 3.4. *For any $T > 0$, suppose f and g are smooth functions with $f(0) = g(0) = 0$. Then*

$$(3.1) \qquad \mathcal{I}_t^1 (2f\mathcal{I}_t^{\frac{2}{3}\alpha} f - (\mathcal{I}_t^{\frac{\alpha}{3}} f)^2)|_{t=T} \geq 0,$$

$$(3.2) \qquad \mathcal{I}_t^1 (2(\mathcal{I}_t^{\frac{\alpha}{3}} g - \mathcal{I}_t^{\frac{2}{3}\alpha} f)f - g^2)|_{t=T} \leq 0.$$

Proof. For any $T > 0$, we set $F(t) = f(t)\mathbb{1}_{[0,T]}, G(t) = g(t)\mathbb{1}_{[0,T]}(t)$, where $\mathbb{1}_{[0,T]}(t)$ is the characteristic function of $[0, T]$. We may then extend the integration domain as follows:

$$
\begin{aligned}
\mathcal{I}_t^1 (2f\mathcal{I}_t^{\frac{2}{3}\alpha} f - (\mathcal{I}_t^{\frac{\alpha}{3}} f)^2)|_{t=T} &= \mathcal{I}_t^1 (2F\mathcal{I}_t^{\frac{2}{3}\alpha} F - (\mathcal{I}_t^{\frac{\alpha}{3}} F)^2)|_{t=T} \\
&= \int_0^{+\infty} (2F\mathcal{I}_t^{\frac{2}{3}\alpha} F - (\mathcal{I}_t^{\frac{\alpha}{3}} F)^2) \mathrm{d}t.
\end{aligned}
$$

We now employ the Plancherel theorem to obtain

$$\int_0^{+\infty} (2F\mathcal{I}_t^{\frac{2}{3}\alpha}F - (\mathcal{I}_t^{\frac{\alpha}{3}}F)^2)\mathrm{d}t$$

$$= \frac{1}{2\pi}\int_{-\infty}^{+\infty}(2(i\xi)^{-\frac{2}{3}\alpha} - |\xi|^{-\frac{2}{3}\alpha})\left|\hat{F}(i\xi)\right|^2\mathrm{d}\xi$$

$$= \frac{1}{2\pi}\int_0^{+\infty}\left[(2(i\xi)^{-\frac{2}{3}\alpha} - |\xi|^{-\frac{2}{3}\alpha}) + (2(-i\xi)^{-\frac{2}{3}\alpha} - |\xi|^{-\frac{2}{3}\alpha})\right]\left|\hat{F}(i\xi)\right|^2\mathrm{d}\xi$$

$$= \frac{1}{2\pi}\int_0^{+\infty}2(2\cos\frac{\pi\alpha}{3} - 1)|\xi|^{-\frac{2\alpha}{3}}\left|\hat{F}(i\xi)\right|^2\mathrm{d}\xi$$

$$\geq 0,$$

where we have used the fact that $1 < 2\cos\frac{\pi\alpha}{3} < 2$ for $0 < \alpha < 1$ and (3.1) is proved. In addition, we have

$$\mathcal{I}_t^1(2(\mathcal{I}_t^{\frac{\alpha}{3}}g - \mathcal{I}_t^{\frac{2}{3}\alpha}f)f - g^2)|_{t=T}$$

$$= \int_0^{+\infty}\left[2(\mathcal{I}_t^{\frac{\alpha}{3}}G - \mathcal{I}_t^{\frac{2}{3}\alpha}F)F - G^2\right]\mathrm{d}t$$

$$\leq \int_0^{+\infty}\left[2F\mathcal{I}_t^{\frac{\alpha}{3}}G - (\mathcal{I}_t^{\frac{\alpha}{3}}F)^2 - G^2\right]\mathrm{d}t$$

$$= \frac{1}{2\pi}\int_{-\infty}^{+\infty}\left(2(i\xi)^{-\frac{\alpha}{3}}\hat{G}(i\xi)\bar{\hat{F}}(i\xi) - |\xi|^{-\frac{2\alpha}{3}}\left|\hat{F}(i\xi)\right|^2 - \left|\hat{G}(i\xi)\right|^2\right)\mathrm{d}\xi$$

$$\leq -\frac{1}{2\pi}\int_{-\infty}^{+\infty}\left(\left|\hat{G}(i\xi)\right| - |\xi|^{-\frac{\alpha}{3}}\left|\hat{F}(i\xi)\right|\right)^2\mathrm{d}\xi$$

$$\leq 0.$$

Here the first inequality follows from (3.1) and the second equality follows from the Plancherel theorem again. $\square$

Theorem 3.5. *The IBVP* (2.20)–(2.24) *is L^2-stable. More precisely, for $0 < t \leq T$, the following estimate holds:*

$$(3.3)\qquad \int_0^t \|u(\cdot,\tau)\|^2\,\mathrm{d}\tau \leq \mathcal{I}_t^\alpha\left(\frac{t^{1-\alpha}}{\Gamma(2-\alpha)}E_\alpha(t^\alpha)\right)\|u(\cdot,0)\|^2$$

$$+ \mathcal{I}_t^\alpha\left(E_\alpha(t^\alpha)\int_0^t\|f(\cdot,\tau)\|^2\mathrm{d}\tau\right).$$

Proof. Multiplying both sides of (2.20) with $2u$, integrating x from x_l to x_r, and applying integration by parts, we obtain

$$(3.4)\quad 2\int_{x_l}^{x_r}u\,{}_0^C\mathcal{D}_t^\alpha u\mathrm{d}x = -2\int_{x_l}^{x_r}(uu_{xx} - \frac{1}{2}u_x^2)_x\mathrm{d}x + \int_{x_l}^{x_r}2uf\mathrm{d}x$$

$$= (2uu_{xx} - u_x^2)(x_l,t) - (2uu_{xx} - u_x^2)(x_r,t) + \int_{x_l}^{x_r}2uf\mathrm{d}x.$$

The exact ABCs (2.22)–(2.24) can be rewritten as follows:

$$u(x_r,t) = -\mathcal{I}_t^{\frac{2\alpha}{3}}u_{xx}(x_r,t), \quad u_x(x_r,t) = \mathcal{I}_t^{\frac{\alpha}{3}}u_{xx}(x_r,t),$$

$$u(x_l,t) = -\mathcal{I}_t^{\frac{2\alpha}{3}}u_{xx}(x_l,t) + \mathcal{I}_t^{\frac{\alpha}{3}}u_x(x_l,t),$$

where the second equality follows from the differentiation of (2.23). Replacing $u(x_l, t)$, $u(x_r, t)$ and $u_x(x_r, t)$ in (3.4) by the above integrals, we have

$$2 \int_{x_l}^{x_r} u \, {}^C_0\mathcal{D}^\alpha_t u \, \mathrm{d}x = \left[2(\mathcal{I}^{\frac{\alpha}{3}}_t u_x - \mathcal{I}^{\frac{2}{3}\alpha}_t u_{xx}) u_{xx} - u_x^2 \right] (x_l, t)$$

$$- \left[2u_{xx} \mathcal{I}^{\frac{2}{3}\alpha}_t u_{xx} - (\mathcal{I}^{\frac{\alpha}{3}}_t u_{xx})^2 \right] (x_r, t) + 2 \int_{x_l}^{x_r} f u \, \mathrm{d}x \mathrm{d}\tau.$$

Integrating both sides of the above equation over $[0, t]$ and then applying Lemmas 3.1 and 3.4, we obtain

$$\mathcal{I}^1_t \, {}^C_0\mathcal{D}^\alpha_t \int_{x_l}^{x_r} u^2 \mathrm{d}x \leq 2 \int_0^t \int_{x_l}^{x_r} f u \, \mathrm{d}x \mathrm{d}\tau.$$

The applications of the Lemma 3.3 and the Cauchy-Schwarz inequality yield

$$(3.5) \qquad \mathcal{I}^{1-\alpha}_t \int_{x_l}^{x_r} u^2 \mathrm{d}x \leq \frac{t^{1-\alpha}}{\Gamma(2-\alpha)} \int_{x_l}^{x_r} u(x,0)^2 \mathrm{d}x$$

$$(3.6) \qquad + \int_0^t \int_{x_l}^{x_r} u^2 \mathrm{d}x \mathrm{d}\tau + \int_0^t \int_{x_l}^{x_r} f^2 \mathrm{d}x \mathrm{d}\tau.$$

Let $v(t) := \mathcal{I}^{1-\alpha}_t \left(\int_{x_l}^{x_r} u^2 \mathrm{d}x \right)$ and $a(t) := \frac{t^{1-\alpha}}{\Gamma(2-\alpha)} \int_{x_l}^{x_r} u_0^2(x) \mathrm{d}x + \int_0^t \int_{x_l}^{x_r} f^2(x,t) \mathrm{d}x \mathrm{d}\tau$. Using the property of the Riemann-Liouville integral $\mathcal{I}^\alpha_t (\mathcal{I}^\beta_t) g(t) = \mathcal{I}^{\alpha+\beta}_t g(t)$ for $\alpha, \beta \in \mathbb{R}^+$, we may rewrite $\int_0^t \int_{x_l}^{x_r} u^2 \mathrm{d}x \mathrm{d}\tau$ as follows:

$$\int_0^t \int_{x_l}^{x_r} u^2 \mathrm{d}x \mathrm{d}\tau = \mathcal{I}^1_t \int_{x_l}^{x_r} u^2 \mathrm{d}x = \mathcal{I}^\alpha_t (\mathcal{I}^{1-\alpha}_t \int_{x_l}^{x_r} u^2 \mathrm{d}x) = \mathcal{I}^\alpha_t v(t).$$

Hence, (3.5) can be rewritten as follows:

$$(3.7) \qquad v(t) \leq a(t) + \mathcal{I}^\alpha_t v(t) = a(t) + \frac{1}{\Gamma(\alpha)} \int_0^t (t - \tau)^{\alpha-1} v(\tau) \mathrm{d}\tau.$$

Obviously $a(t)$ is nondecreasing. A direct application of Lemma 3.2 to (3.7) with $b(t) = \frac{1}{\Gamma(\alpha)}$ leads to

$$(3.8) \qquad v(t) \leq a(t) E_\alpha(t^\alpha).$$

Applying the operator $\mathcal{I}^\alpha_t$ on both sides of (3.8) leads to the desired result (3.3). $\square$

Lemma 3.6. *For any $T > 0$, suppose f and g are smooth functions with $f(0) = g(0) = 0$. Then*

$$\mathcal{I}^1_t (2f \, {}^C_0\mathcal{D}^{\frac{2}{3}\alpha}_t f - ({}^C_0\mathcal{D}^{\frac{\alpha}{3}}_t f)^2)|_{t=T} \geq 0,$$

$$\mathcal{I}^1_t (2({}^C_0\mathcal{D}^{\frac{\alpha}{3}}_t g - {}^C_0\mathcal{D}^{\frac{2}{3}\alpha}_t f) f - g^2)|_{t=T} \leq 0.$$

Proof. Let $F(t) = f(t) \mathbb{1}_{[0,T]}, G(t) = g(t) \mathbb{1}_{[0,T]}(t)$. Then we have

$$\mathcal{I}^1_t (2f \, {}^C_0\mathcal{D}^{\frac{2}{3}\alpha}_t f - ({}^C_0\mathcal{D}^{\frac{\alpha}{3}}_t f)^2)|_{t=T} = \int_0^{+\infty} (2F \, {}^C_0\mathcal{D}^{\frac{2}{3}\alpha}_t F - ({}^C_0\mathcal{D}^{\frac{\alpha}{3}}_t F)^2) \mathrm{d}t.$$

Applying the Plancherel theorem yields

$$\int_0^{+\infty} (2F\, {}_0^C\mathcal{D}_t^{\frac{2}{3}\alpha}F - ({}_0^C\mathcal{D}_t^{\frac{\alpha}{3}}F)^2)\mathrm{d}t$$

$$= \frac{1}{2\pi}\int_{-\infty}^{+\infty}(2(i\xi)^{\frac{2}{3}\alpha} - |\xi|^{\frac{2}{3}\alpha})\left|\hat{F}(i\xi)\right|^2\mathrm{d}\xi$$

$$= \frac{1}{2\pi}\int_0^{+\infty}2(2\cos\frac{\pi\alpha}{3} - 1)|\xi|^{\frac{2\alpha}{3}}\left|\hat{F}(i\xi)\right|^2\mathrm{d}\xi \geq 0.$$

In addition, we have

$$\mathcal{I}_t^1(2({}_0^C\mathcal{D}_t^{\frac{\alpha}{3}}g - {}_0^C\mathcal{D}_t^{\frac{2}{3}\alpha}f)f - g^2)|_{t=T}$$

$$= \int_0^{+\infty}\left[2({}_0^C\mathcal{D}_t^{\frac{\alpha}{3}}G - {}_0^C\mathcal{D}_t^{\frac{2}{3}\alpha}F)F - G^2\right]\mathrm{d}t$$

$$\leq \int_0^{+\infty}\left[2F\, {}_0^C\mathcal{D}_t^{\frac{\alpha}{3}}G - ({}_0^C\mathcal{D}_t^{\frac{\alpha}{3}}F)^2 - G^2\right]\mathrm{d}t$$

$$= \frac{1}{2\pi}\int_{-\infty}^{+\infty}\left(2(i\xi)^{\frac{\alpha}{3}}\hat{G}(i\xi)\bar{\hat{F}}(i\xi) - |\xi|^{\frac{2\alpha}{3}}\left|\hat{F}(i\xi)\right|^2 - \left|\hat{G}(i\xi)\right|^2\right)\mathrm{d}\xi$$

$$\leq -\frac{1}{2\pi}\int_{-\infty}^{+\infty}\left(\left|\hat{G}(i\xi)\right| - |\xi|^{\frac{\alpha}{3}}\left|\hat{F}(i\xi)\right|\right)^2\mathrm{d}\xi \leq 0,$$

where we have used Lemma 3.1 in the first inequality. The proof is complete. $\square$

Analogous to the proof of Theorem 3.5 with Lemma 3.6 playing the role of Lemma 3.4, we obtain the stability result for the IBVP (2.25)–(2.29), which is summarized in the following theorem.

Theorem 3.7. *The IBVP (2.25)–(2.29) is L^2-stable in the sense of (3.3).*

4. A FINITE DIFFERENCE SCHEME

In this section, we first construct a finite difference (FD) scheme for the IBVP (2.25)–(2.29). We then show that the FD scheme is unconditionally stable in the L^2-norm. Finally, we apply the fast algorithm for the evaluation of the Caputo derivative developed in [15] to reduce the computational and storage cost.

4.1. Construction of the finite difference scheme. We first observe that the PDE and boundary conditions contain the spatial derivatives up to the third order. If we discretize the third-order derivative in the PDE via the central difference for the interior points and the spatial derivatives in boundary conditions via one-sided finite differences, there is a mismatch between the interior points and the boundary points. And our numerical experiments show that the resulting scheme is only conditionally stable even though the scheme is implicit. Thus, one needs a more careful and delicate analysis in order to obtain an unconditionally stable FD scheme. For this, we introduce an auxiliary variable $v(x, t) = u_x(x, t)$ and rewrite

the IBVP (2.25)–(2.29) as follows:

$$(4.1) \qquad {}^C_0\mathcal{D}^\alpha_t u(x,t) + v_{xx}(x,t) = f(x,t), \quad x \in \Omega_c,\ t \in (0,T],$$

$$(4.2) \qquad v = u_x, \quad x \in \Omega_c,\ t \in (0,T],$$

$$(4.3) \qquad u(x,0) = u_0(x), \quad x \in \Omega_c,$$

$$(4.4) \qquad v_x(x_r,t) = {}^C_0\mathcal{D}^{\frac{2\alpha}{3}}_t u(x_r,t), \quad t \in (0,T],$$

$$(4.5) \qquad v(x_r,t) = -{}^C_0\mathcal{D}^{\frac{\alpha}{3}}_t u(x_r,t), \quad t \in (0,T],$$

$$(4.6) \qquad v_x(x_l,t) - {}^C_0\mathcal{D}^{\frac{\alpha}{3}}_t v(x_l,t) + {}^C_0\mathcal{D}^{\frac{2\alpha}{3}}_t u(x_l,t) = 0, \quad t \in (0,T].$$

We first discuss the discretization of the Caputo fractional derivative in time. For a given integer N, let $\{t_k\}_{k=0}^N$ be a partition of $[0,T]$ with $t_k = k\Delta t$ and $\Delta t_k = t_k - t_{k-1} = \frac{T}{N}$. For a mesh function $U = \{U^k = u(t_k)|0 \le k \le N\}$, we approximate $u(t)$ via a piecewise linear polynomial with $\{t_k\}_{k=0}^N$ as the interpolation nodes and obtain the following $L1$ discretization for approximating the Caputo fractional derivative:

$$(4.7) \qquad D^\alpha_t U^k = \frac{\Delta t^{-\alpha}}{\Gamma(2-\alpha)} \left[a_0^{(\alpha)} U^k - \sum_{l=1}^{k-1} (a_{k-l-1}^{(\alpha)} - a_{k-l}^{(\alpha)}) U^l - a_{k-1}^{(\alpha)} U^0 \right]$$

for $1 \le k \le N$. Here $a_l^{(\alpha)} = (l+1)^{1-\alpha} - l^{1-\alpha}$. The accuracy of the $L1$ discretization is given as follows.

Lemma 4.1 (See [28]). *Suppose that $u(t) \in C^2[0,T]$. Let*

$$R(u(t_k)) := {}^C_0\mathcal{D}^\alpha_t u(t)|_{t=t_k} - D^\alpha_t U^k, \quad 1 \le k \le N.$$

Then

$$\left| R^k u \right| \le \frac{1}{\Gamma(2-\alpha)} \left[\frac{1-\alpha}{12} + \frac{2^{2-\alpha}}{2-\alpha} - (1+2^{-\alpha}) \right] \max_{0 \le t \le t_k} |u''(t)| \Delta t^{2-\alpha}.$$

Next, we discuss the discretization of spatial derivatives and boundary conditions. For a given integer M, let $\{x_i\}_{i=0}^M$ be an equispaced partition of (x_l, x_r) with $x_i = x_l + ih$ and $h = (x_r - x_l)/M$. Denote $U^n_i = u(x_i, t_n)$, $f^n_i = f(x_i, t_n)$, and

$$(4.8)\ \ \delta_x U^k_{i+\frac{1}{2}} = \frac{1}{h}\left(U^k_{i+1} - U^k_i\right), \quad U^k_{i+\frac{1}{2}} = \frac{1}{2}\left(U^k_i + U^k_{i+1}\right),\ 0 \le i \le M-1,$$

$$(4.9)\ \ \delta^2_x U^k_i = \frac{1}{h}\left(\delta_x U^k_{i+\frac{1}{2}} - \delta_x U^k_{i-\frac{1}{2}}\right) = \frac{1}{h^2}\left(U^k_{i+1} - 2U^k_i + U^k_{i-1}\right),\ 1 \le i \le M-1.$$

We also denote $V^n_i = v(x_i, t_n)$ and define $\delta_x V^k_{i+\frac{1}{2}}$, $V^k_{i+\frac{1}{2}}$, and $\delta^2_x V^k_i$ similarly as in (4.8) and (4.9). We apply these second-order central differences to approximate the spatial derivatives in (4.1) and (4.2) at interior nodes. As for the boundary nodes, we note that the Taylor theorem leads to the following lemma.

Lemma 4.2 (See [10]). *Suppose that $y(x) \in C^3(\Omega_c)$. Then*

$$y''(x_0) - \frac{2}{h}\left[\frac{y(x_1) - y(x_0)}{h} - y'(x_0)\right] = -\frac{h}{3}y^{(3)}(x_0 + \theta_1 h), \quad \theta_1 \in (0,1),$$

$$y''(x_M) - \frac{2}{h}\left[y'(x_M) - \frac{y(x_M) - y(x_{M-1})}{h}\right] = -\frac{h}{3}y^{(3)}(x_M - \theta_2 h), \quad \theta_2 \in (0,1).$$

We now discuss the discretization at the right end point x_M. The boundary condition (4.5) can be discretized via the $L1$ discretization of the Caputo derivative directly since it does not contain any spatial derivative. To obtain another discrete condition at x_M, we discretize the Caputo derivatives in the PDE (4.1) and the boundary condition (4.4) to obtain

$$D_t^\alpha U_M^k + v_{xx}(x_M, t_k) \approx f_M^k,$$

$$v_x(x_M, t_k) \approx D_t^{\frac{2\alpha}{3}} U_M^k.$$

The second equation in Lemma 4.2 leads to

$$v_{xx}(x_M, t_k) \approx \frac{2}{h} \left[v_x(x_M, t_k) - \delta_x V_{M-\frac{1}{2}}^k \right].$$

Combining the three equations above to eliminate v_x and v_{xx}, we have

$$(4.10) \qquad D_t^\alpha U_M^k + \frac{2}{h} \left(D_t^{\frac{2\alpha}{3}} U_M^k - \delta_x V_{M-\frac{1}{2}}^k \right) \approx f_M^k.$$

Similarly, we can derive the discrete condition at x_0. To summarize, we have the following approximation for the IBVP (4.1)–(4.6):

$$(4.11) \qquad D_t^\alpha U_i^k + \delta_x^2 V_i^k = f_i^k + T_i^k, \quad 1 \le i \le M-1, \ 1 \le k \le N,$$

$$(4.12) \qquad V_{i+\frac{1}{2}}^k = \delta_x U_{i+\frac{1}{2}}^k + Q_{i+\frac{1}{2}}^k, \quad 0 \le i \le M-1, \ 1 \le k \le N,$$

$$(4.13) \qquad D_t^{\frac{\alpha}{3}} U_M^k = -V_M^k + R_M^k, \quad 1 \le k \le N,$$

$$(4.14) \qquad D_t^\alpha U_M^k + \frac{2}{h} \left(D_t^{\frac{2\alpha}{3}} U_M^k - \delta_x V_{M-\frac{1}{2}}^k \right) = f_M^k + T_M^k, \quad 1 \le k \le N,$$

$$(4.15) \qquad D_t^\alpha U_0^k + \frac{2}{h} \left(\delta_x V_{\frac{1}{2}}^k - D_t^{\frac{\alpha}{3}} V_0^k + D_t^{\frac{2\alpha}{3}} U_0^k \right) = f_0^k + T_0^k, \quad 1 \le k \le N.$$

That is, (4.11) follows from the $L1$ discretization of the Caputo derivative and central difference discretization of v_{xx} of the PDE (4.1); (4.12) is the central difference discretization of the auxillary equation (4.2); (4.13) follows from the $L1$ discretization of the Caputo derivative of the boundary condition (4.5); (4.14) follows from (4.10); and (4.15) follows from a similar derivation for the left end point x_0 which combines the PDE (4.1), the boundary condition (4.6), and the first equation in Lemma 4.2.

Here the truncation errors are defined by the formulas

$$T_i^k = \left[D_t^\alpha U_i^k - {}_0^C\mathcal{D}_t^\alpha u(x_i, t_k) \right] + \left[\delta_x^2 V_i^k - v_{xx}(x_i, t_k) \right], \ 1 \le i \le M-1, \ 1 \le k \le N,$$

$$T_0^k = \left[D_t^\alpha U_0^k - {}_0^C\mathcal{D}_t^\alpha u(x_0, t_k) \right] + \left[\frac{2}{h} \left(\delta_x V_{\frac{1}{2}}^k - v_x(x_0, t_k) \right) - v_{xx}(x_0, t_k) \right]$$

$$+ \frac{2}{h} \left[{}_0^C\mathcal{D}_t^{\frac{\alpha}{3}} v(x_0, t_k) - D_t^{\frac{\alpha}{3}} V_0^k \right] - \frac{2}{h} \left[{}_0^C\mathcal{D}_t^{\frac{2\alpha}{3}} u(x_0, t_k) - D_t^{\frac{2\alpha}{3}} U_0^k \right], \ 1 \le k \le N,$$

$$T_M^k = \left[D_t^\alpha U_M^k - {}_0^C\mathcal{D}_t^\alpha u(x_M, t_k) \right] + \left[\frac{2}{h} \left(v_x(x_M, t_k) - \delta_x V_{M-\frac{1}{2}}^k \right) - v_{xx}(x_M, t_k) \right]$$

$$- \frac{2}{h} \left[{}_0^C\mathcal{D}_t^{\frac{2\alpha}{3}} u(x_M, t_k) - D_t^{\frac{2\alpha}{3}} U_M^k \right], \ 1 \le k \le N,$$

$$R_M^k = D_t^{\frac{\alpha}{3}} U_M^k - {}_0^C\mathcal{D}_t^{\frac{\alpha}{3}} u(x_M, t_k), \quad 1 \le k \le N.$$

$$Q_{i+\frac{1}{2}}^k = u_x(x_{i+\frac{1}{2}}, t_k) - \delta_x U_{i+\frac{1}{2}}^k + V_{i+\frac{1}{2}}^k - v(x_{i+\frac{1}{2}}, t_k), \ 0 \le i \le M-1, \ 1 \le k \le N.$$

By Lemma 4.1 and the Taylor theorem, for $u \in C_{x,t}^{5,2}\left(\Omega_c \times [0, t_k]\right)(1 \leq k \leq N)$ we have

$$(4.16) \qquad \left|T_i^k\right| \leq c(\Delta t^{2-\alpha} + h^2), \quad 1 \leq i \leq M - 1,\ 1 \leq k \leq N,$$

$$(4.17) \qquad \left|T_0^k\right| \leq c(\Delta t^{2-\alpha} + h + \Delta t^{2-\frac{2}{3}\alpha}/h), \quad 1 \leq k \leq N,$$

$$(4.18) \qquad \left|T_M^k\right| \leq c(\Delta t^{2-\alpha} + h + \Delta t^{2-\frac{2}{3}\alpha}/h), \quad 1 \leq k \leq N,$$

$$(4.19) \qquad \left|R_M^k\right| \leq c(\Delta t^{2-\frac{1}{3}\alpha}), \quad 1 \leq k \leq N,$$

$$(4.20) \qquad \left|Q_{i+\frac{1}{2}}^k\right| \leq ch^2, \quad 0 \leq i \leq M - 1,\ 1 \leq k \leq N.$$

Finally, omitting the truncation terms $T_i^k\ (0 \leq i \leq M, 1 \leq k \leq N)$, $R_M^k\ (1 \leq k \leq N)$ and $Q_{i+\frac{1}{2}}^k\ (1 \leq i \leq M - 1, 1 \leq k \leq N)$, we obtain the following finite difference scheme for solving the IBVP (2.25)–(2.29):

$$(4.21) \qquad D_t^\alpha U_i^k + \delta_x^2 V_i^k = f_i^k, \quad 1 \leq i \leq M - 1,\ 1 \leq k \leq N,$$

$$(4.22) \qquad D_t^\alpha U_0^k + \frac{2}{h}\left(\delta_x V_{\frac{1}{2}}^k - D_t^{\frac{\alpha}{3}} V_0^k + D_t^{\frac{2\alpha}{3}} U_0^k\right) = f_0^k, \quad 1 \leq k \leq N,$$

$$(4.23) \qquad D_t^\alpha U_M^k + \frac{2}{h}\left(D_t^{\frac{2\alpha}{3}} U_M^k - \delta_x V_{M-\frac{1}{2}}^k\right) = f_M^k, \quad 1 \leq k \leq N,$$

$$(4.24) \qquad D_t^{\frac{\alpha}{3}} U_M^k = -V_M^k, \quad 1 \leq k \leq N,$$

$$(4.25) \qquad V_{i+\frac{1}{2}}^k = \delta_x U_{i+\frac{1}{2}}^k, \quad 0 \leq i \leq M - 1,\ 1 \leq k \leq N.$$

Remark 4.3. As compared with the direct FD scheme mentioned at the beginning of this subsection, our FD scheme has second-order accuracy for v at interior points and first-order accuracy at boundary points. Since $v = u_x$, this implies third-order accuracy for u at interior points and second-order accuracy at boundary points. Thus, our FD scheme has a higher order of accuracy and better stability property.

4.2. **Stability analysis of the finite difference scheme.** We now show that the FD scheme (4.21)–(4.25) is unconditionally stable. We first recall that the Riemann-Liouville fractional derivative is defined by the formula (see, for example, [24])

$$\,_0^R\mathcal{D}_t^\alpha u(x, t) = \frac{1}{\Gamma(1-\alpha)} \frac{d}{dt} \int_0^t \frac{u(x, s)}{(t - s)^\alpha} ds, \quad 0 < \alpha < 1.$$

For any $1 \leq n \leq N$, suppose that the piecewise constant function of a mesh vector $(0, u^1, u^2, \ldots, u^n)$ with zero initial value is defined by the formula

$$u(t) := \begin{cases} u^k, & t \in [t_{k-1}, t_k),\ 1 \leq k \leq n, \\ 0, & t \notin [t_0, t_n). \end{cases}$$

The following lemma connects the Riemann-Liouville fractional derivative of a piecewise constant function with the $L1$ discretization (4.7) of the corresponding mesh vector with zero initial data.

Lemma 4.4. *Let $u(t)$ and $v(t)$ be the piecewise constant functions of the mesh vectors $(0, u^1, u^2, \ldots, u^n)$ and $(0, v^1, v^2, \ldots, v^n)$ with zero initial values, respectively.*

Then $u, v \in H^{\frac{\alpha}{3}}(\mathbb{R}^+)$. Furthermore,

(4.26)
$$\mathcal{I}_t^1 \left(u(t) {}_0^R\mathcal{D}_t^{\frac{\alpha}{3}} v(t) \right) \big|_{t=t_n} = \Delta t \sum_{k=1}^n u^k D_t^{\frac{\alpha}{3}} v^k,$$

$$\mathcal{I}_t^1 \left(u(t) {}_0^R\mathcal{D}_t^{\frac{2\alpha}{3}} u(t) \right) \big|_{t=t_n} = \Delta t \sum_{k=1}^n u^k D_t^{\frac{2\alpha}{3}} u^k,$$

and

(4.27)
$$\mathcal{I}_t^1 \left({}_0^R\mathcal{D}_t^{\frac{\alpha}{3}} u(t) \right)^2 \big|_{t=t_n} \geq \Delta t \sum_{k=1}^n (D_t^{\frac{\alpha}{3}} u^k)^2.$$

Proof. The identities in (4.26) can be proved via straightforward calculation. The details are presented in [29].

As for the inequality (4.27), we first apply Jensen's inequality to obtain

(4.28) $\quad \mathcal{I}_t^1 \left({}_0^R\mathcal{D}_t^{\frac{\alpha}{3}} u(t) \right)^2 \big|_{t=t_n} = \dfrac{1}{\Gamma(1-\frac{\alpha}{3})^2} \displaystyle\sum_{k=1}^n \int_{t_{k-1}}^{t_k} \left(\dfrac{\mathrm{d}}{\mathrm{d}t} \int_0^t \dfrac{u(s)}{(t-s)^{\frac{\alpha}{3}}} \mathrm{d}s \right)^2 \mathrm{d}t$

$$\geq \dfrac{\Delta t^{-1}}{\Gamma(1-\frac{\alpha}{3})^2} \sum_{k=1}^n \left(\int_{t_{k-1}}^{t_k} \dfrac{\mathrm{d}}{\mathrm{d}t} \int_0^t \dfrac{u(s)}{(t-s)^{\frac{\alpha}{3}}} \mathrm{d}s \mathrm{d}t \right)^2.$$

We then observe that

(4.29)
$$\dfrac{1}{\Gamma(1-\frac{\alpha}{3})} \int_{t_{k-1}}^{t_k} \dfrac{\mathrm{d}}{\mathrm{d}t} \int_0^t \dfrac{u(s)}{(t-s)^{\frac{\alpha}{3}}} \mathrm{d}s \mathrm{d}t$$

$$= \mathcal{I}_t^1 \left({}_0^R\mathcal{D}_t^{\frac{\alpha}{3}} u(t) \right) \big|_{t=t_k} - \mathcal{I}_t^1 \left({}_0^R\mathcal{D}_t^{\frac{\alpha}{3}} u(t) \right) \big|_{t=t_{k-1}}$$

$$= \Delta t \sum_{l=1}^k D_t^{\frac{\alpha}{3}} u^l - \Delta t \sum_{l=1}^{k-1} D_t^{\frac{\alpha}{3}} u^l$$

$$= \Delta t D_t^{\frac{\alpha}{3}} u^k,$$

where the first equality follows from the fact that $\mathcal{I}_t^1$ is simply the integration operator from 0 to t and the second equality follows from (4.26). Combining (4.28) and (4.29), we obtain (4.27). $\qquad\square$

Proceeding as in the proof of Lemma 3.6, we obtain the following lemma.

Lemma 4.5. *For any $T > 0$, suppose $f, g \in H^{\frac{\alpha}{3}}(0, T)$. Then*

(4.30)
$$\mathcal{I}_t^1 (2f {}_0^R\mathcal{D}_t^{\frac{2}{3}\alpha} f - ({}_0^R\mathcal{D}_t^{\frac{\alpha}{3}} f)^2)|_{t=T} \geq 0,$$

(4.31)
$$\mathcal{I}_t^1 (2({}_0^R\mathcal{D}_t^{\frac{\alpha}{3}} g - {}_0^R\mathcal{D}_t^{\frac{2}{3}\alpha} f)f - g^2)|_{t=T} \leq 0.$$

The next lemma can be found in [10].

Lemma 4.6. *For any mesh functions $g = \{g^k | 0 \leq k \leq N\}$ defined on $\Omega_t = \{t_k | 0 \leq k \leq N\}$, the following inequality holds:*

(4.32) $\quad \Delta t \displaystyle\sum_{k=1}^n (D_t^\alpha g^k) g^k \geq \dfrac{t_n^{-\alpha}}{2\Gamma(1-\alpha)} \Delta t \sum_{k=1}^n (g^k)^2 - \dfrac{t_n^{1-\alpha}}{2\Gamma(2-\alpha)} (g^0)^2, \quad 1 \leq n \leq N.$

Let $\mathbb{V} = \{v | v = (v_0, v_1, \ldots, v_M)\}$. For any $U, V \in \mathbb{V}$, we define the inner product and norm as

$$(U, V) = h\left(\frac{1}{2}U_0 V_0 + \sum_{i=1}^{M-1} U_i V_i + \frac{1}{2}U_M V_M\right), \quad \|U\| = \sqrt{(U,U)}.$$

We now present the main theoretical result on the stability of the FD scheme.

Theorem 4.7. *The finite difference scheme* (4.21)–(4.25) *is unconditionally stable with respect to the initial data and the source term. That is,*

$$(4.33) \quad \Delta t \sum_{k=1}^{n} \|U^k\|^2 \leq \frac{2t_n}{1-\alpha} \|U^0\|^2 + 4t_n^{2\alpha}\Gamma(1-\alpha)^2 \Delta t \sum_{k=1}^{n} \|f^k\|^2, \quad 1 \leq n \leq N.$$

Proof. We multiply both sides of (4.21) by hU_i^k, and then sum up for i from 1 to $M-1$; we then multiply both sides of (4.22) and (4.23) by $\frac{h}{2}U_0^k$ and $\frac{h}{2}U_M^k$, respectively; finally we add up these equations to obtain

$$(4.34) \quad \left(D_t^\alpha U^k, U^k\right) + \sum_{i=1}^{M-1} h\delta_x^2 V_i^k \cdot U_i^k + \delta_x V_{\frac{1}{2}}^k \cdot U_0^k - \delta_x V_{M-\frac{1}{2}}^k \cdot U_M^k$$

$$- D_t^{\frac{\alpha}{3}} V_0^k \cdot U_0^k + D_t^{\frac{2\alpha}{3}} U_0^k \cdot U_0^k + D_t^{\frac{2\alpha}{3}} U_M^k \cdot U_M^k = (f^k, U^k).$$

We then use (4.25) to simplify the second term to the fourth term of the left side in (4.34),

$$(4.35) \quad \sum_{i=1}^{M-1} h\delta_x^2 V_i^k \cdot U_i^k + \delta_x V_{\frac{1}{2}} \cdot U_0^k - \delta_x V_{M-\frac{1}{2}} \cdot U_M^k$$

$$= \sum_{i=1}^{M-1} \left(\delta_x V_{i+\frac{1}{2}}^k - \delta_x V_{i-\frac{1}{2}}^k\right) \cdot U_i^k + \delta_x V_{\frac{1}{2}} U_0^k - \delta_x V_{M-\frac{1}{2}} U_M^k$$

$$= \sum_{i=1}^{M} \delta_x V_{i-\frac{1}{2}}^k (U_{i-1}^k - U_i^k) = \sum_{i=1}^{M} \left(V_{i-1}^k - V_i^k\right) \delta_x U_{i-\frac{1}{2}}^k$$

$$= \sum_{i=1}^{M} \frac{\left(V_{i-1}^k\right)^2 - \left(V_i^k\right)^2}{2} = \frac{1}{2}(V_0^k)^2 - \frac{1}{2}(V_M^k)^2.$$

Substituting (4.35) and (4.24) into (4.34), we obtain

$$(4.36) \quad \left(D_t^\alpha U^k, U^k\right) + \frac{1}{2}(V_0^k)^2 - D_t^{\frac{\alpha}{3}} V_0^k \cdot U_0^k + D_t^{\frac{2\alpha}{3}} U_0^k \cdot U_0^k$$

$$- \frac{1}{2}\left(D_t^{\frac{\alpha}{3}} U_M^k\right)^2 + D_t^{\frac{2\alpha}{3}} U_M^k \cdot U_M^k = (f^k, U^k).$$

Multiplying Δt on both sides of the (4.36), summing up for k from 1 to n, and applying Lemma 4.4, we obtain

$$(4.37) \quad \sum_{k=1}^{n} \Delta t \left(D_t^\alpha U^k, U^k\right) + \mathcal{I}_t^1 \left(\frac{1}{2}(V_0)^2 - ({}_0^R\mathcal{D}_t^{\frac{\alpha}{3}} V_0)U_0 + ({}_0^R\mathcal{D}_t^{\frac{2\alpha}{3}} U_0)U_0\right)\Big|_{t=t_n}$$

$$+ \mathcal{I}_t^1 \left(({}_0^R\mathcal{D}_t^{\frac{2\alpha}{3}} U_M)U_M - \frac{1}{2}\left({}_0^R\mathcal{D}_t^{\frac{\alpha}{3}} U_M\right)^2\right)\Big|_{t=t_n} \leq \sum_{k=1}^{n} \Delta t(f^k, U^k).$$

Here U_0, V_0, U_M are piecewise constant functions of the mesh vectors $(U_0^0, U_0^1, \ldots,$ $U_0^n)$, $(V_0^0, V_0^1, \ldots, V_0^n)$, and $(U_M^0, U_M^1, \ldots, U_M^n)$, respectively; and we have used the fact that $U_M^0 = U_0^0 = V_0^0 = 0$ by the assumption that the initial data are compactly supported.

By the inequality (4.31), the second term on the left side of (4.37) is nonnegative; by the inequality (4.30), the third term on the left side of (4.37) is nonnegative. Thus,

$$(4.38) \qquad \sum_{k=1}^{n} \Delta t \left(D_t^\alpha U^k, U^k \right) \le \sum_{k=1}^{n} \Delta t (f^k, U^k).$$

Applying the inequality (4.32) to estimate the left side of (4.38), we have

$$(4.39) \qquad \frac{t_n^{-\alpha}}{2\Gamma(1-\alpha)} \Delta t \sum_{k=1}^{n} \left\| U^k \right\|^2 \le \frac{t_n^{1-\alpha}}{2\Gamma(2-\alpha)} \left\| U^0 \right\|^2 + \sum_{k=1}^{n} \Delta t (f^k, U^k).$$

Now the Cauchy-Schwarz inequality yields

$$(4.40) \qquad (f^k, U^k) \le \left\| f^k \right\| \cdot \left\| U^k \right\|$$

$$\le t_n^\alpha \Gamma(1-\alpha) \left\| f^k \right\|^2 + \frac{t_n^{-\alpha}}{4\Gamma(1-\alpha)} \left\| U^k \right\|^2.$$

Finally, combining (4.39) with (4.40) and simplifying the resulting expression, we obtain (4.33). $\qquad\square$

4.3. Acceleration of the finite difference scheme.

The direct implementation of the FD scheme (4.21)–(4.25) is very expensive in both the computational and storage cost. This is because the Caputo derivative is a nonlocal operator and its $L1$ discretization (or any consistent discretization) contains a summation that involves all values of the solution up to the current time. Hence, one needs to store all previous solution values and the total cost of evaluating the $L1$ discretization at each spatial point is $O(N^2)$ with N the total number of time steps.

We apply the fast algorithm for the evaluation of the Caputo fractional derivative in [15] to reduce the computational and storage cost. In order to make the paper more or less self-contained, we present here a short summary of the algorithm in [15]. We first split the fractional Caputo derivative into a sum of local part and history part

$$\,_0^C\mathcal{D}_t^\alpha u(t)|_{t=t_k} = \frac{1}{\Gamma(1-\alpha)} \int_{t_{k-1}}^{t_k} \frac{u'(s)ds}{(t_k-s)^\alpha} + \frac{1}{\Gamma(1-\alpha)} \int_0^{t_{k-1}} \frac{u'(s)ds}{(t_k-s)^\alpha}$$

$$(4.41) \qquad := C_l(t_k) + C_h(t_k).$$

For the local part $C_l(t_k)$, we apply the $L1$ approximation in the form

$$(4.42) \qquad C_l(t_k) \approx \frac{u(t_k) - u(t_{k-1})}{\Delta t_k \Gamma(1-\alpha)} \int_{t_{k-1}}^{t_k} \frac{1}{(t_k-s)^\alpha} ds = \frac{u(t_k) - u(t_{k-1})}{\Delta t_k^\alpha \Gamma(2-\alpha)}.$$

For the history part $C_h(t_k)$, we first perform integration by parts to obtain

$$(4.43) \qquad C_h(t_k) = \frac{1}{\Gamma(1-\alpha)} \left[\frac{u(t_{k-1})}{\Delta t_k^\alpha} - \frac{u(t_0)}{t_k^\alpha} - \alpha \int_0^{t_{k-1}} \frac{u(s)ds}{(t_k-s)^{1+\alpha}} \right].$$

Obviously, the most work is on the evaluation of the convolution integral with the kernel $\frac{1}{t^{1+\alpha}}$ on the right side of (4.43). It has been shown in [15] that there exists an efficient sum-of-exponentials approximation for $\frac{1}{t^{1+\alpha}}$ for any given time interval

TABLE 1. Number of exponentials $N_{\exp}$ needed to approximate $t^{-1-\alpha}$ with fixed $\Delta t = 10^{-3}$ for $\alpha = 0.5$.

$\varepsilon \diagdown \frac{T}{\Delta t}$	10^3	10^4	10^5	10^6
10^{-3}	28	30	35	38
10^{-6}	42	47	47	51
10^{-9}	49	55	64	67

$[\Delta t_k, T]$ with a prescribe absolute error ε. To be more precise, there exist positive real numbers s_i and w_i $(i = 1, \ldots, N_{\exp})$ such that

$$(4.44) \qquad \left| \frac{1}{t^{1+\alpha}} - \sum_{i=1}^{N_{\exp}} \omega_i e^{-s_i t} \right| \leq \varepsilon, \quad t \in [\Delta t, T];$$

and the number of exponentials $N_{\exp}$ needed is of the order (see Table 1 for an example of the actual number of exponentials needed)

$$O\left(\log \frac{1}{\varepsilon} \left(\log \log \frac{1}{\varepsilon} + \log \frac{T}{\Delta t} \right) + \log \frac{1}{\Delta t} \left(\log \log \frac{1}{\varepsilon} + \log \frac{1}{\Delta t} \right) \right).$$

That is, for fixed precision ε, we have $N_{\exp} = O(\log N)$ for $T \gg 1$ or $N_{\exp} = O(\log^2 N)$ for $T \approx 1$ assuming that $N = \frac{T}{\Delta t}$.

Replacing the convolution kernel $\frac{1}{t^{1+\alpha}}$ in (4.43) by its sum-of-exponentials approximation in (4.44), we obtain

$$(4.45) \qquad C_h(t_k) \approx \frac{1}{\Gamma(1-\alpha)} \left[\frac{u(t_{k-1})}{\Delta t_k^\alpha} - \frac{u(t_0)}{t_k^\alpha} - \alpha \sum_{i=1}^{N_{\exp}} \omega_i U_{\text{hist,i}}(t_k) \right],$$

where $U_{\text{hist,i}}(t_k)$ is defined by

$$(4.46) \qquad U_{\text{hist,i}}(t_k) = \int_0^{t_{k-1}} e^{-(t_k-\tau)s_i} u(\tau) d\tau.$$

The reduction of the computational and storage cost relies on the fact that $U_{\text{hist,i}}(t_k)$ satisfies a simple recurrence relation

$$(4.47) \qquad U_{\text{hist,i}}(t_k) = e^{-s_i \Delta t_k} U_{\text{hist,i}}(t_{k-1}) + \int_{t_{k-2}}^{t_{k-1}} e^{-s_i(t_k-\tau)} u(\tau) d\tau$$

with $U_{\text{hist,i}}(t_0) = 0$ for $i = 1, \ldots, N_{\exp}$. The integral on the right-hand side of (4.47) can be calculated by a linear approximation of u followed with a product integration. That is,

$$(4.48) \qquad \int_{t_{k-2}}^{t_{k-1}} e^{-s_i(t_k-\tau)} u(\tau) d\tau \approx \frac{e^{-s_i \Delta t_k}}{s_i^2 \Delta t_{k-1}} \left[(e^{-s_i \Delta t_{k-1}} - 1 + s_i \Delta t_{k-1}) U^{k-1} \right.$$
$$\left. + (1 - e^{-s_i \Delta t_{k-1}} - e^{-s_i \Delta t_{k-1}} s_i \Delta t_{k-1}) U^{k-2} \right].$$

Thus, one only needs $O(1)$ cost to compute $U_{\text{hist,i}}(t_k)$ at each step as $U_{\text{hist,i}}(t_{k-1})$ is already computed and stored. As there are $N_{\exp}$ history modes altogether, the cost of evaluating the Caputo derivative at each time step is $O(N_{\exp})$. That is, a reduction from $O(N)$ to $O(\log N)$ or $O(\log^2 N)$.

To summarize, the fast evaluation of the Caputo derivative can be implemented by the formula

$$(4.49) \quad {}_0^C\mathcal{D}_t^\alpha U^k \approx \frac{U^k - U^{k-1}}{\Delta t_k^\alpha \Gamma(2-\alpha)} + \frac{1}{\Gamma(1-\alpha)} \left[\frac{U^{k-1}}{\Delta t_k^\alpha} - \frac{U^0}{t_k^\alpha} - \alpha \sum_{i=1}^{N_{\exp}} \omega_i U_{\mathrm{hist},i}(t_k) \right]$$

$$=: {}^F\!D_t^\alpha U^k, \quad \text{for} \quad k > 0,$$

where $U_{\mathrm{hist},i}(t_k)$ is evaluated via (4.47) and (4.48). Finally, replacing the $L1$ discretization $D_t^\alpha U^k$ by its fast version ${}^F\!D_t^\alpha U^k$ in the FD scheme (4.21)–(4.25), we obtain an accelerated FD scheme as follows:

$$(4.50) \qquad {}^F\!D_t^\alpha U_i^k + \delta_x^2 V_i^k = f_i^k, \quad 1 \leq i \leq M-1, \ 1 \leq k \leq N,$$

$$(4.51) \qquad {}^F\!D_t^\alpha U_0^k + \frac{2}{h}\left(\delta_x V_{\frac{1}{2}}^k - {}^F\!D_t^{\frac{\alpha}{3}} V_0^k + {}^F\!D_t^{\frac{2\alpha}{3}} U_0^k \right) = f_0^k, \quad 1 \leq k \leq N,$$

$$(4.52) \qquad {}^F\!D_t^\alpha U_M^k + \frac{2}{h}\left({}^F\!D_t^{\frac{2\alpha}{3}} U_M^k - \delta_x V_{M-\frac{1}{2}}^k \right) = f_M^k, \quad 1 \leq k \leq N,$$

$$(4.53) \qquad {}^F\!D_t^{\frac{\alpha}{3}} U_M^k = -V_M^k, \quad 1 \leq k \leq N,$$

$$(4.54) \qquad V_{i+\frac{1}{2}}^k = \delta_x U_{i+\frac{1}{2}}^k, \quad 0 \leq i \leq M-1, \ 1 \leq k \leq N.$$

Remark 4.8. The fast algorithm relies on the fact that the convolution with the exponential kernel can be evaluated in linear time since it is equivalent to solving an ordinary differential equation (ODE). Thus it can be applied to adaptive time marching scheme as well. The only penalty here is that the number of exponentials will increase slightly due to the decrease of the smallest time step.

Remark 4.9. Another fast algorithm for the evaluation of the fractional derivative has been proposed in [4], where the compression is carried out in the Laplace domain, and the convolution with an exponential kernel is computed by solving the equivalent ODE with some one-step A-stable scheme.

Remark 4.10. Both the $L1$ discretization $D_t^\alpha U^k$ and the fast algorithm ${}^F\!D_t^\alpha U^k$ approximate $u(t)$ by a piecewise polynomial and then apply the product integration. Therefore, the difference is very minor and can in fact be made arbitrarily small if the prescribed precision ε is set to a small number, say, close to machine precision. In our numerical experiments, we have not observed any significant differences between the FD scheme (4.21)–(4.25) and its fast version (4.50)–(4.54) in both accuracy and stability.

5. Numerical examples

We now report results of numerical experiments which demonstrate the effectiveness of our exact ABCs and offer quantitative features of the finite difference schemes (4.21)–(4.25) and (4.50)–(4.54) in various aspects: convergence order, the computational complexity, and the dependence on ε. To examine the convergence orders, we define the error norm and convergence order by the formulas

$$E(h, \Delta t) = \sqrt{\sum_{k=1}^{m} \Delta t \, \|e^k\|^2}, \quad r_t = \log_2 \frac{E(h, \Delta t)}{E(h, \Delta t/2)}, \quad r_s = \log_2 \frac{E(h, \Delta t)}{E(h/2, \Delta t)}.$$

In order to obtain smooth reference solutions in Example 5.1, we set the right-hand side of the first equation in (1.1) based on the given exact smooth solutions. As we

will see, both schemes (4.21)–(4.25) and (4.50)–(4.54) have the same convergence order $h^4 + \Delta t^{2-\alpha}$ due to the negligible influence of the SOE approximation error ε on the accuracy of the fast algorithm; but the fast algorithm is much faster than the direct method even when N is of moderate size. We will illustrate the effectiveness of ABCs. On the one hand, no reflection wave from artificial boundaries can be seen from the evolution graph of the solutions. On the other hand, we also check the energy defined by $E(t) = \int_{x_l}^{x_r} u^2(x,t)dx$ on the bounded domain to verify the effectiveness of our ABCs, which can be numerically calculated via the trapezoidal rule.

Example 5.1. We consider the exact solution of the form $u(x,t) = \exp(-x^2)t^2$ for the problem (1.1), which leads to the source function $f(x,t) = \frac{2}{\Gamma(3-\alpha)}t^{2-\alpha}\exp(-x^2)$ $+ t^2\exp(-x^2)(12x - 8x^3)$. In our computation, we set the computational domain $\Omega_c = (-6,6)$, final time $T = 1$ and the tolerance precision $\varepsilon = 10^{-12}$ for the SOE approximation.

Fixing $h = 10^{-3}$ and varying Δt from $\frac{1}{20}$ to $\frac{1}{160}$, Table 2 illustrates the errors $E(h,\Delta t)$ and the convergence order of $\Delta t^{2-\alpha}$ for both schemes (4.21)–(4.25) and (4.50)–(4.54) in cases of $\alpha = 0.2, 0.4, 0.6$ and 0.8. Next, fixing $\Delta t = 10^{-4}$ and varying h from $\frac{12}{27}$ to $\frac{12}{64}$, Table 3 illustrates the errors $E(h,\Delta t)$ and the convergence order of h^4 in space for both methods in cases of $\alpha = 0.2, 0.4, 0.6$ and 0.8.

Tables 2 and 3 show that both the fast algorithm and the direct method produce the same overall convergence order of $h^4 + \Delta t^{2-\alpha}$. We plot the difference of solutions of these two schemes for $\varepsilon = 10^{-7}, 10^{-8}, 10^{-9}$, and 10^{-10}, respectively. As we can see in Figure 1, the difference in the solutions of the two schemes becomes smaller and smaller when ε gets smaller and smaller.

TABLE 2. Example 1: The error and convergence order in time for fast and direct schemes, the spatial mesh size is fixed at $h = 10^{-3}$.

Δt	Fast scheme		Direct scheme		Fast scheme		Direct scheme	
	$E(h,\Delta t)$	r_t	$E(h,\Delta t)$	r_t	$E(h,\Delta t)$	r_t	$E(h,\Delta t)$	r_t
	$\alpha = 0.2$				$\alpha = 0.4$			
1/20	6.55385108e-04	1.71	6.55385108e-04	1.71	2.24705517e-03	1.55	2.24705517e-03	1.55
1/40	2.00843055e-04	1.72	2.00843055e-04	1.72	7.65737566e-04	1.56	7.65737566e-04	1.56
1/80	6.09797829e-05	1.73	6.09797829e-05	1.73	2.59174561e-04	1.57	2.59174561e-04	1.57
1/160	1.83606636e-05		1.83606636e-05		8.72173249e-05		8.72173249e-05	
	$\alpha = 0.6$				$\alpha = 0.8$			
1/20	5.90307640e-03	1.38	5.90307640e-03	1.38	1.38884744e-02	1.20	1.38884744e-02	1.20
1/40	2.26680324e-03	1.39	2.26680324e-03	1.39	6.04731488e-03	1.20	6.04731488e-03	1.20
1/80	8.67621912e-04	1.39	8.67621912e-04	1.39	2.63569499e-03	1.20	2.63569499e-03	1.20
1/160	3.31144112e-04		3.31144112e-04		1.14869621e-03		1.14869621e-03	

We now check the computational cost of both methods. For this, we calculate the CPU time for $N = 2 \times 10^4, 4 \times 10^4, \ldots, 1.2 \times 10^5$ with $\alpha = 0.5, M = 30$ fixed. Figure 2 clearly shows the $O(N^2)$ complexity of the direct method and the $O(N)$ complexity of the fast method.

In summary, this example provides a detailed comparison between the fast algorithm and the direct method. Specifically, we have been able to understand the superiority of our fast algorithm when N is large enough. We can use the fast

TABLE 3. Example 1: The error, convergence order in space and CPU time for fast and direct schemes, the time step size is fixed at $\Delta t = 10^{-4}$.

h	Fast scheme		Direct scheme		Fast scheme		Direct scheme	
	$E(h, \Delta t)$	r_s	$E(h, \Delta t)$	r_s	$E(h, \Delta t)$	r_s	$E(h, \Delta t)$	r_s
	$\alpha = 0.2$				$\alpha = 0.4$			
12/27	9.65355988e-04	4.24	9.65355988e-04	4.24	9.64031334e-04	4.24	9.64031334e-04	4.24
12/36	2.85181520e-04	4.13	2.85181520e-04	4.13	2.84755576e-04	4.13	2.84755576e-04	4.13
12/48	8.69658395e-05	4.07	8.69658395e-05	4.07	8.68307687e-05	4.07	8.68307687e-05	4.07
12/64	2.69650162e-05		2.69650162e-05		2.69230020e-05		2.69230020e-05	
CPU(s)	34.50		3.19e+02		34.42		3.34e+02	
	$\alpha = 0.6$				$\alpha = 0.8$			
12/27	9.63086232e-04	4.24	9.63086232e-04	4.24	9.63498568e-04	4.24	9.63498738e-04	4.24
12/36	2.84459020e-04	4.13	2.84459020e-04	4.13	2.84788157e-04	4.11	2.84787989e-04	4.11
12/48	8.67497706e-05	4.07	8.67497706e-05	4.07	8.72903060e-05	3.92	8.72890018e-05	3.92
12/64	2.69232642e-05		2.69232642e-05		2.82430370e-05		2.82382760e-05	
CPU(s)	34.53		3.30e+02		35.06		3.30e+02	
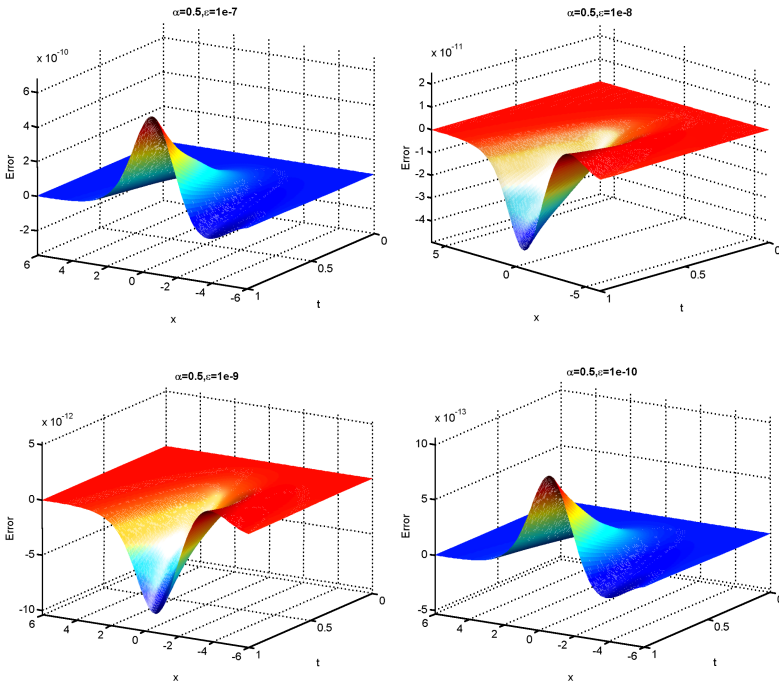
FIGURE 1. Example 1: The evolution of the difference (i.e., Error = $^{F}U_h^n - {}^{D}U_h^n$) in the solutions to the direct scheme (4.21)–(4.24) (denote by $^{D}U_h^n$) and to the fast scheme (4.50)–(4.53) (denote by $^{F}U_h^n$) for $\varepsilon = $ 1e-7, 1e-8, 1e-9, 1e-10, respectively. In the calculation, we set $M = 120$, $N = 1000$, and $\alpha = 0.5$.

evaluation to obtain almost the same accuracy as the direct method, and yet, the fast algorithm is much faster and saves the computational memory for long time simulation.
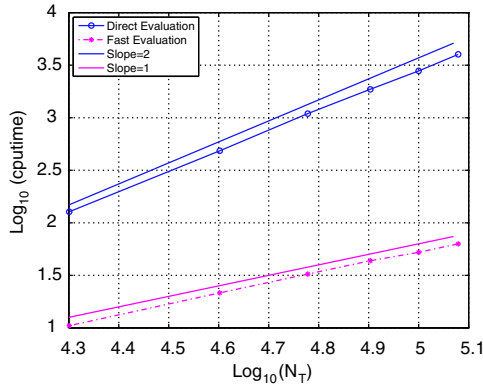
FIGURE 2. Example 1: The CPU time of different N with $M = 30$.

Example 5.2. We now use our fast algorithm to analyze some features of the solution to (1.1) and verify the effectiveness of our ABCs. We choose the source term $f(x,t) = 0$ and initial value $u_0(x) = \exp(-8(x-5)^2)$. In our computation, we set $\varepsilon = 10^{-10}$, and $\Omega_c = (-8, 8)$. Note that using Fourier transform, we can compute the exact solution $u_{\text{exact}}(x, t)$. In details, using Fourier transform in space variable to the first equation in (1.1), we get

$$_0^C\mathcal{D}_t^\alpha \hat{u}(\xi, t) - i\xi^3 \hat{u}(\xi, t) = 0,$$

where ξ is the Fourier variable. Then the solution to above equation is

$$\hat{u}_{\text{exact}}(\xi, t) = \hat{u}_0 E_\alpha(i\xi^3 t^\alpha),$$

where E_α is the Mittag-Leffler function defined in Lemma 3.2. Then we have the exact solution of the problem using the inverse Fourier transform. We compute the reference solution in a larger domain using 30000 points in space.

From Example 5.1, we find the convergence rate in space is $O(h^4)$. To confirm this result, we test the spatial convergence rate in this case. From Table 4, we can observe that the convergence rate is still $O(h^4)$.

TABLE 4. Example 2: The errors and convergence orders in space with $\alpha = 0.99$, $T = 0.001$ and $\Delta t = h^4$.

h	$\alpha = 0.99$	
	$E(h, \Delta t)$	r_s
1/10	3.7373804042e-05	4.0810
1/20	2.1970772051e-06	4.0800
1/30	4.0840637549e-07	4.2186
1/40	1.2188775601e-07	

Figure 3 shows the evolution of the solutions by comparing with the reference solutions for different values of α. As can be seen in Figure 3, there are no artificial reflections from the boundaries, which demonstrates the accuracy of our ABCs.

We also plot energies in the computational domain in Figure 4 for different values of α. We observe that the energy decays as the wave moves away from

(a) $\alpha = 0.5$
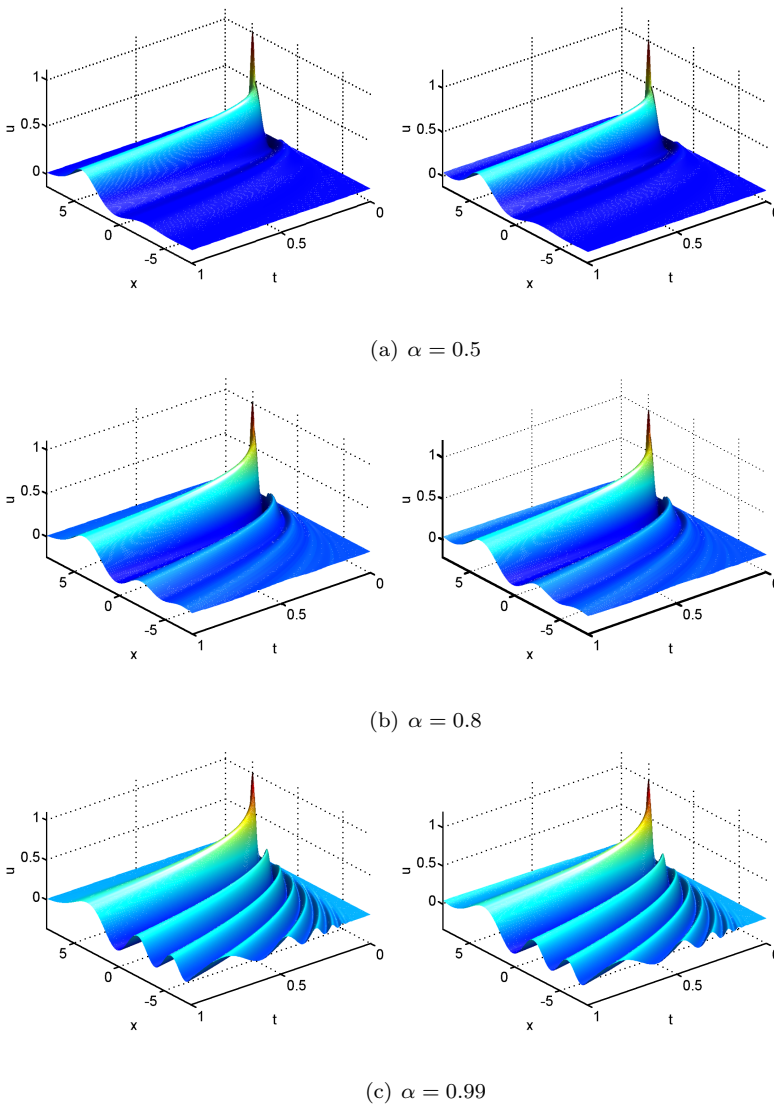

(b) $\alpha = 0.8$

(c) $\alpha = 0.99$

FIGURE 3. Example 2: The evolutions of the reference solution (left) and numerical solution (right). In the calculation of numerical solutions, we set $\Delta t = 10^{-3}$ and $h = 10^{-3}$.

the computational domain, which indicates again the stability of our ABCs for long-time simulations.

Example 5.3. We now check the effectiveness of our ABCs in the high-frequency region. We consider the high-frequency wave generated by $f(x,t) = 0$ and $u_0(x) = \exp(-8(x-5)^2)\sin(50x\pi/4)$. We calculate the reference solution using finer mesh sizes in a larger domain to minimize the influence of ABCs, and calculate the numerical solutions via the fast algorithm. In the calculation, we set $\epsilon = 10^{-12}$ and choose different lengths of the computational interval Ω_c and different final times
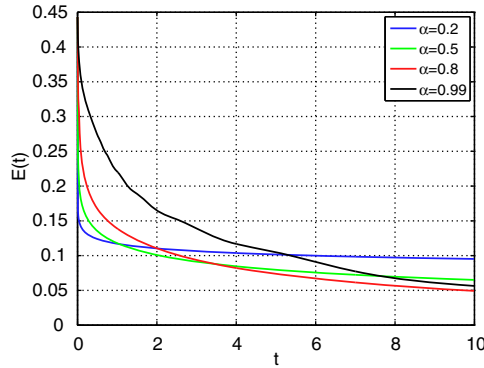
FIGURE 4. Example 2: The evolution of the energy of the wave remained in the bounded computational domain for different values of α. In this calculation, $M = 2000$, $N = 5000$, $x_l = -8$, $x_r = 8$, and $T = 10$.

T for various values of α. Figure 5 shows the evolutions of the numerical solutions, which move away from the center of this wave package.

To further investigate the effectiveness of our ABCs, Figure 6 shows the reference solutions and numerical solutions as well as their errors, and Figure 7 shows the energy remained in the computational domains for different values of α. We observe that the errors are very small in Figure 6 and the energy decays in Figure 7. We remark again that no instability has been observed in any of our computations.

Example 5.4. Our fast algorithm can be easily applied to the case of nonuniform time step size. We have observed from the first example that the convergence order in time is $2 - \alpha$ when the solution is sufficiently smooth; but the rate of the convergence deteriorates significantly when an initial layer is present near $t = 0$, as shown in the third column of Table 5. In this example, we will use graded time steps to capture the singular behaviour of the solution near $t = 0$. We consider the exact solution $u(x, t) = E_\alpha(-t^\alpha)e^{-x^2}$ for the problem (1.1). The source function is $f(x, t) = E_\alpha(-t^\alpha)e^{-x^2}(-1 + 12x - 8x^3)$ and the initial data is $u_0(x) = e^{-x^2}$. In the calculation, we take the computational domain $\Omega_c = (-5, 5)$, final time $T = 1$, and the tolerance precision $\varepsilon = 10^{-10}$ for the SOE approximation. Then the grid in time is taken to be

$$t_k = \left(\frac{k}{N}\right)^\gamma T,$$

where γ is a parameter to be chosen. When $\gamma = 1$, the grid is uniform; when $\gamma > 1$, the grid is nonuniform with finer mesh near $t = 0$. Table 5 shows the errors and convergence order in time for $\gamma = 1$, $\gamma = 2$ and $\gamma = 5/2$. We observe that while the uniform temporal grid (i.e., $\gamma = 1$) does not resolve the initial layer and thus has poor convergence rate, the graded mesh steps with $\gamma = 2$ and $\gamma = 5/2$ capture the initial layer very well and the convergence rate of the overall scheme is close to the theoretical value.
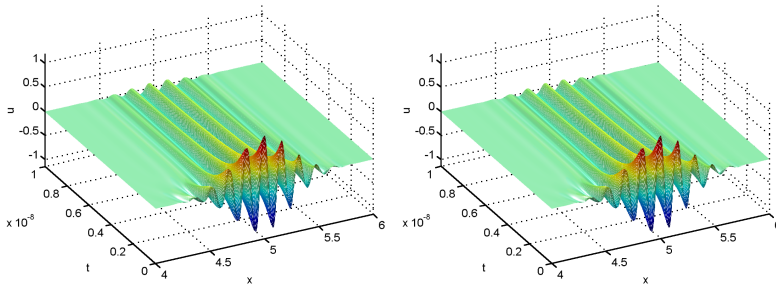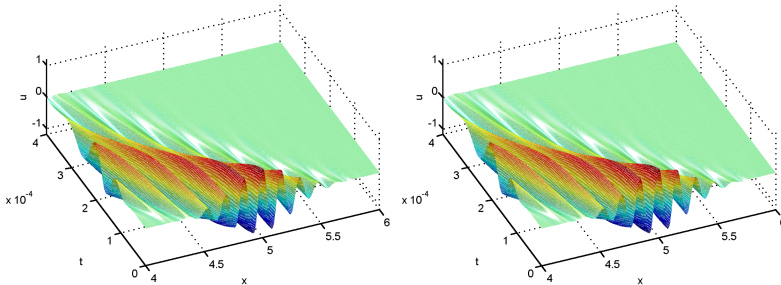
(a) $\alpha = 0.5$
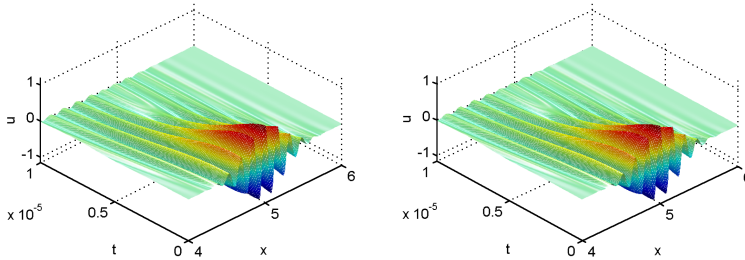
(b) $\alpha = 0.8$
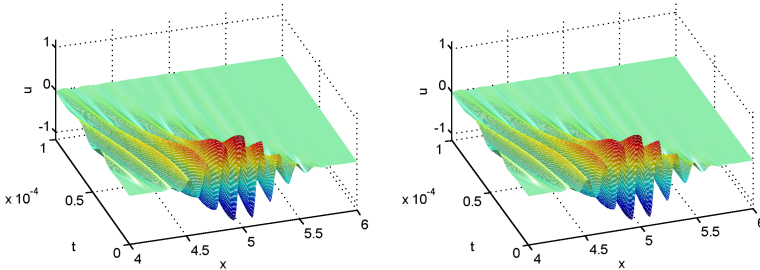
(c) $\alpha = 0.9$

(d) $\alpha = 0.99$

FIGURE 5. Example 3: The evolution of the reference solution (left) and the numerical solution (right). In this calculation, $x_l = -6$, $x_r = 6$, $h = 10^{-3}$, $N = 1000$. $T = 1 \times 10^{-8}$ for $\alpha = 0.5$, $T = 1 \times 10^{-5}$ for $\alpha = 0.8$, $T = 1 \times 10^{-4}$ for $\alpha = 0.9$, $T = 4 \times 10^{-4}$ for $\alpha = 0.99$. $\Delta t = T/N$.
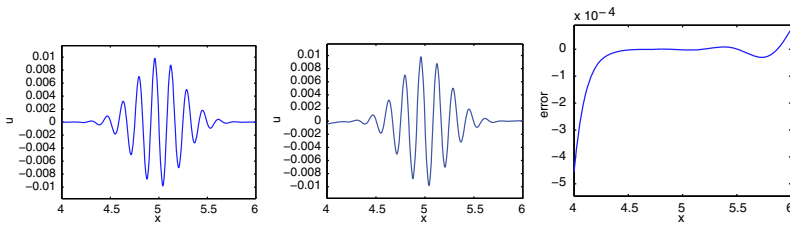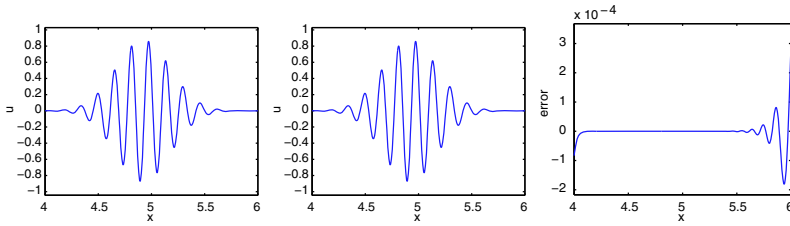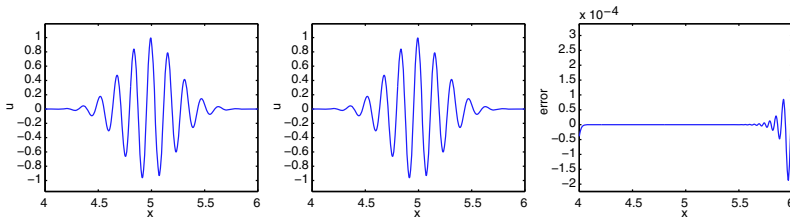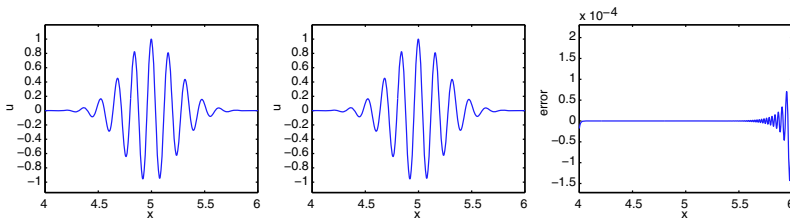
(a) $\alpha = 0.2$

(b) $\alpha = 0.5$

(c) $\alpha = 0.8$

(d) $\alpha = 0.99$

FIGURE 6. Example 3: Reference solutions (left), numerical solutions (center) and the errors between them (right) at $T = 1 \times 10^{-6}$. In the calculation of numerical solutions, we take $M = 1000$, $N = 1000$ to ensure Δt and h are same with the ones in the calculation of reference solutions.
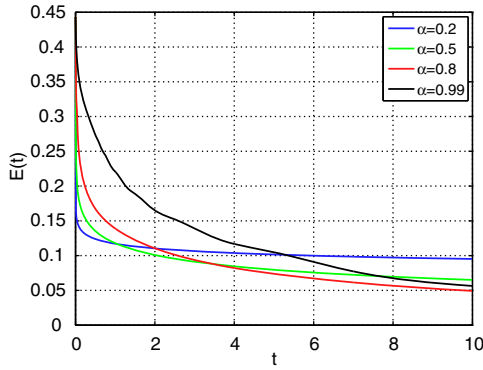
FIGURE 7. Example 3: The evolution of the energy of the wave remained in the bounded computational domain for different values of α. In this calculation, we take $M = 1000$, $N = 1000$, $x_l = 0$, $x_r = 10$ and $T = 4 \times 10^{-4}$.

TABLE 5. Example 4: The errors and convergence orders with $\alpha = 0.5$ and $M = 10000$ in time for various values of γ.

N	$\gamma = 1$	order	$\gamma = 2$	order	$\gamma = 5/2$	order
10	4.18154e-02		1.86953e-02		1.52165e-02	
20	2.42127e-02	0.79	8.09866e-03	1.21	6.15820e-03	1.31
40	1.36471e-02	0.83	3.36761e-03	1.27	2.38934e-03	1.37
80	7.54121e-03	0.86	1.35930e-03	1.31	9.01284e-04	1.41
160	4.10562e-03	0.88	5.36724e-04	1.34	3.33587e-04	1.43
time(s)	8.46720e+00		9.17506e+00		1.21342e+01	

6. Conclusions

In this paper, we have presented an efficient and stable numerical method for solving the linearized time fractional KdV equation. We have derived the exact artificial boundary conditions and showed that resulting initial-boundary value problem is L^2-stable. An unconditionally stable finite difference is then constructed for the discretization of the initial-boundary value problem. Finally, the fast algorithm for the evaluation of the Caputo fractional derivative is incorporated into the stable finite difference scheme, which leads to a robust numerical algorithm with nearly optimal complexity. To be more precise, our fast algorithm reduces the storage requirement from $O(MN)$ to $O(MN_{\exp})$ and the overall computational cost from $O(MN^2)$ to $O(MNN_{\exp})$ as compared with the direct method, where $N_{\exp}$ is $\log^d N$ with either $d = 1$ or $d = 2$. This provides a practical way for the long-time simulation of the linearized time-fractional KdV equation.

Acknowledgments

References

[1] A. A. Alikhanov, *A priori estimates for solutions of boundary value problems for equations of fractional order*, Differ. Uravn. **46** (2010), no. 5, 658–664, DOI 10.1134/S0012266110050058; English transl., Differ. Equ. **46** (2010), no. 5, 660–666. MR2797545

[2] B. Alpert, L. Greengard, and T. Hagstrom, *Rapid evaluation of nonreflecting boundary kernels for time-domain wave propagation*, SIAM J. Numer. Anal. **37** (2000), no. 4, 1138–1164, DOI 10.1137/S0036142998336916. MR1756419

[3] B. Alpert, L. Greengard, and T. Hagstrom, *Nonreflecting boundary conditions for the time-dependent wave equation*, J. Comput. Phys. **180** (2002), no. 1, 270–296, DOI 10.1006/jcph.2002.7093. MR1913093

[4] D. Baffet and J. S. Hesthaven, *A Laplace transform based kernel reduction scheme for fractional differential equations*, https://infoscience.epfl.ch/record/212955, 2016.

[5] C. Besse, M. Ehrhardt, and I. Lacroix-Violet, *Discrete artificial boundary conditions for the linearized Korteweg–de Vries equation*, Numer. Methods Partial Differential Equations **32** (2016), no. 5, 1455–1484, DOI 10.1002/num.22058. MR3535627

[6] G. Beylkin and L. Monzón, *Approximation by exponential sums revisited*, Appl. Comput. Harmon. Anal. **28** (2010), no. 2, 131–149, DOI 10.1016/j.acha.2009.08.011. MR2595881

[7] H. Brunner, L. Ling, and M. Yamamoto, *Numerical simulations of 2D fractional subdiffusion problems*, J. Comput. Phys. **229** (2010), no. 18, 6613–6622, DOI 10.1016/j.jcp.2010.05.015. MR2660323

[8] S. A. El-Wakil, E. M. Abulwafa, M. A. Zahran, and A. A. Mahmoud, *Time-fractional KdV equation: formulation and solution using variational methods*, Nonlinear Dynam. **65** (2011), no. 1-2, 55–63, DOI 10.1007/s11071-010-9873-5. MR2812008

[9] M. K. Fung, *KdV equation as an Euler-Poincaré equation*, Chinese J. Phys. **35** (1997), no. 6, 789–796. MR1613273

[10] G.-h. Gao and Z.-z. Sun, *The finite difference approximation for a class of fractional sub-diffusion equations on a space unbounded domain*, J. Comput. Phys. **236** (2013), 443–460, DOI 10.1016/j.jcp.2012.11.011. MR3020065

[11] H. Han and X. Wu, *Artificial Boundary Method*, Springer, Heidelberg, Tsinghua University Press, Beijing, 2013. MR3137472

[12] S. Jiang, *Fast Evaluation of the Nonreflecting Boundary Conditions for the Schrödinger Equation*, Ph.D. thesis, Courant Institute of Mathematical Sciences, New York University, New York, 2001.

[13] S. Jiang and L. Greengard, *Fast evaluation of nonreflecting boundary conditions for the Schrödinger equation in one dimension*, Comput. Math. Appl. **47** (2004), no. 6-7, 955–966, DOI 10.1016/S0898-1221(04)90079-X. MR2060329

[14] S. Jiang and L. Greengard, *Efficient representation of nonreflecting boundary conditions for the time-dependent Schrödinger equation in two dimensions*, Comm. Pure Appl. Math. **61** (2008), no. 2, 261–288, DOI 10.1002/cpa.20200. MR2368376

[15] S. Jiang, J. Zhang, Q. Zhang, and Z. Zhang, *Fast evaluation of the Caputo fractional derivative and its applications to fractional diffusion equations*, Commun. Comput. Phys. **21** (2017), 650–678.

[16] B. Jin, R. Lazarov, and Z. Zhou, *Two fully discrete schemes for fractional diffusion and diffusion-wave equations with nonsmooth data*, SIAM J. Sci. Comput. **38** (2016), no. 1, A146–A170, DOI 10.1137/140979563. MR3449907

[17] L. José, O. Eugene, and S. Martin, *Error analysis of a finite difference method for a time-fractional advection-diffusion equation*, to appear, 2015.

[18] A. A. Kilbas, H. M. Srivastava, and J. J. Trujillo, *Theory and Applications of Fractional Differential Equations*, North-Holland Mathematics Studies, vol. 204, Elsevier Science B.V., Amsterdam, 2006. MR2218073

[19] D. J. Korteweg and G. de Vries, *On the change of form of long waves advancing in a rectangular canal, and on a new type of long stationary waves*, Philos. Mag. (5) **39** (1895), no. 240, 422–443. MR3363408

[20] T. A. M. Langlands and B. I. Henry, *Fractional chemotaxis diffusion equations*, Phys. Rev. E (3) **81** (2010), no. 5, 051102, 12, DOI 10.1103/PhysRevE.81.051102. MR2736241

[21] J.-R. Li, *A fast time stepping method for evaluating fractional integrals*, SIAM J. Sci. Comput. **31** (2009/10), no. 6, 4696–4714, DOI 10.1137/080736533. MR2594999

[22] R. Metzler and J. Klafter, *The random walk's guide to anomalous diffusion: a fractional dynamics approach*, Phys. Rep. **339** (2000), no. 1, 77, DOI 10.1016/S0370-1573(00)00070-3. MR1809268

[23] S. Momani, *An explicit and numerical solutions of the fractional KdV equation*, Math. Comput. Simulation **70** (2005), no. 2, 110–118, DOI 10.1016/j.matcom.2005.05.001. MR2163618

[24] K. B. Oldham and J. Spanier, *The Fractional Calculus*: *Theory and Applications of Differentiation and Integration to Arbitrary Order*, Mathematics in Science and Engineering, vol. 111, Academic Press, New York-London, 1974. MR0361633

[25] I. Podlubny, *Fractional Differential Equations*: *An Introduction to Fractional Derivatives, Fractional Differential Equations, to Methods of Their Solution and Some of Their Applications*, Mathematics in Science and Engineering, vol. 198, Academic Press, Inc., San Diego, CA, 1999. MR1658022

[26] M. Z. Qin, *Difference schemes for the dispersive equation*, Computing **31** (1983), no. 3, 261–267, DOI 10.1007/BF02263436. MR722326

[27] J. Russell, *Report of the committee on waves*, Rep. Meet. Brit. Assoc. Adv. Sci. 7th Liverpool (1837) 417, John Murray, London.

[28] Z.-z. Sun and X. Wu, *A fully discrete difference scheme for a diffusion-wave system*, Appl. Numer. Math. **56** (2006), no. 2, 193–209, DOI 10.1016/j.apnum.2005.03.003. MR2200938

[29] Z.-z. Sun and X. Wu, *The stability and convergence of a difference scheme for the Schrödinger equation on an infinite domain by using artificial boundary conditions*, J. Comput. Phys. **214** (2006), no. 1, 209–223, DOI 10.1016/j.jcp.2005.09.011. MR2208677

[30] S. V. Tsynkov, *Numerical solution of problems on unbounded domains. A review*, Appl. Numer. Math. **27** (1998), no. 4, 465–532, DOI 10.1016/S0168-9274(98)00025-7. MR1644674

[31] Q. Wang, *Homotopy perturbation method for fractional KdV equation*, Appl. Math. Comput. **190** (2007), no. 2, 1795–1802, DOI 10.1016/j.amc.2007.02.065. MR2339772

[32] G. B. Whitham, *Linear and Nonlinear Waves*, Pure and Applied Mathematics, Wiley-Interscience, New York, London, Sydney, 1974. MR0483954

[33] N. Zabusky and M. Kruskal, *Interactions of solitons in a collisionless plasma and the recurrence of initial states*, Phys. Rev. Lett. **15** (1965), no. 6, 240–243.

[34] W. Zhang, H. Li, and X. Wu, *Local absorbing boundary conditions for a linearized Korteweg-de Vries equation*, Phys. Rev. E **89** (2014), no. 5, 053305.

[35] Y. Zhang, *Formulation and solution to time-fractional generalized Korteweg–de Vries equation via variational methods*, Adv. Difference Equ., posted on 2014, 2014:65, 12, DOI 10.1186/1687-1847-2014-65. MR3359759

[36] C. Zheng, *Approximation, stability and fast evaluation of exact artificial boundary condition for the one-dimensional heat equation*, J. Comput. Math. **25** (2007), no. 6, 730–745. MR2359962

[37] C. Zheng, X. Wen, and H. Han, *Numerical solution to a linearized KdV equation on unbounded domain*, Numer. Methods Partial Differential Equations **24** (2008), no. 2, 383–399, DOI 10.1002/num.20267. MR2382787

Beijing Computational Science Research Center, Beijing 100193, China
  E-mail address: `qianzhang@csrc.ac.cn`

Beijing Computational Science Research Center, Beijing 100193, China
  E-mail address: `jwzhang@csrc.ac.cn`

Department of Mathematical Sciences, New Jersey Institute of Technology, Newark, New Jersey 07102
  E-mail address: `shidong.jiang@njit.edu`

Beijing Computational Science Research Center, Beijing 100193, China — and — Department of Mathematics, Wayne State University, Detroit, Michigan 48202
  E-mail address: `zmzhang@csrc.ac.cn`
  E-mail address: `zzhang@math.wayne.edu`